Selective Alcohol Oxidation with Molecular Oxygen Catalyzed by Os−Cr and Ru−Cr Complexes

Patricia A. Shapley,* Najie Zhang, Jana L. Allen, Douglas H. Pool, and Hong-Chang Liang

Contribution from the Department of Chemistry, University of Illinois, Urbana, Illinois 02168

Received June 22, 1998. Revised Manuscript Received May 17, 1999

Abstract: The heterobimetallic complexes [Y][M(N)R_2(μ-O)$_2$CrO_2] (where Y is either N(*n*-Bu)$_4^+$ or PPh_4^+; M is either Ru or Os; and R is an alkyl or aryl ligand) catalyze the selective oxidation of alcohols with molecular oxygen. The rate of the reaction is higher with a ruthenium-containing complex than with an analogous osmium-containing catalyst. The rate decreases with steric bulk in either the catalyst or substrate. Single-crystal X-ray diffraction studies of [N(*n*-Bu)$_4$][Ru(N)(CH_2SiMe_3)$_2$(μ-O)$_2$CrO_2] and [PPh_4][Os(N)Me(CH_2SiMe_3)(μ-O)$_2$CrO_2] show the chromate group coordinated to each nitrido(dialkyl)metal center through two oxo ligands. The oxidation of benzyl alcohol by [N(*n*-Bu)$_4$][Os(N)(CH_2SiMe_3)$_2$(μ-O)$_2$CrO_2] was examinined in detail. It is first order in alcohol and substrate, and, when oxygen partial pressure is low, the rate depends directly on the O_2 partial pressure. A mechanism in which alcohol coordinates to the osmium center and is oxidized by β-hydrogen elimination is consistent with the data. [N(*n*-Bu)$_4$][Os(N)(CH_2SiMe_3)$_2$(μ-O)$_2$CrO_2] catalyzes the oxidation of dppe with O_2 through a different pathway.

Introduction

Oxidation reactions can increase the number of functional groups and are useful in the synthesis of complex organic molecules. The oxidation of alcohols is an important process.[1] While many metal complexes catalytically convert alcohols to carbonyl compounds, ruthenium compounds are particularly useful for this process.[2−5]

Mechanistic studies demonstrate that metal-mediated alcohol oxidation can proceed through electron transfer to the metal complex, through abstraction of a hydride by the metal oxo unit, or through a concerted β-hydrogen elimination pathway. Complexes of Co(III) oxidize alcohols by an electron-transfer mechanism with a radical intermediate, R_2(OH)C$^\bullet$.[6] In other cases, the alcohol reacts with the metal complex to form an intermediate alkoxide complex. β-Hydrogen elimination produces carbonyl compounds from the alkoxides in *trans*-(RO)-Ir(CO)(PPh_3)$_2$.[7] Ruthenium tetraoxide and related oxo complexes oxidize alcohols by abstracting a hydride, giving an oxygen-stabilized carbocation.[4,5,8] In other studies, the mechanistic data are ambiguous and the pathway may change depending on the substrate, or there may be only partial C−H bond cleavage in the rate-determining step.[9,10]

Secondary oxidants used in metal-catalyzed oxidation of alcohols include dialkyl sulfoxides, $NaIO_4$, NaClO, and H_2O_2. Molecular oxygen can also be used as the secondary oxidant for the oxidation of alcohols.[11,12] In some cases, molecular oxygen reacts with metal complexes to generate catalytically active oxo or peroxo complexes.

Many researchers have prepared heterometallic complexes with the goal of using these in catalysis.[13] Some enzymes use two or more metals in the active site to activate molecular oxygen and oxidize some substrate.[14] Most heterobimetallic complexes are coordinatively saturated and unreactive. In an interesting recent study, Brown et al. found that the presence of a second metal actually impedes alcohol oxidation by ruthenium.[12]

In a brief communication, we reported that the heterobimetallic Os−Cr complexes [N(*n*-Bu)$_4$][Os(N)(CH_2SiMe_3)$_2$(μ-O)$_2$-

(1) (a) G. Cainelli, G.; Cardillo, G. *Chromium Oxidations in Organic Chemistry*; Springer-Verlag: Berlin, 1984. (b) Muzart, J. *Bull. Soc. Chim. Fr.* **1986**, 65−77. (c) Sheldon, R. A.; Kochi, J. K. *Metal Catalyzed Oxidations of Organic Compounds*; Academic Press: New York, 1981; Chapter 6. (d) Wiberg, K. B. *Oxidation in Organic Chemistry*; Academic Press: New York, 1965.

(2) (a) Lima, E. C.; Fenga, P. G.; Romero, J. R.; Degiovani, W. F. *Polyhedron* **1998**, *17*, 313−318. (b) Boelrijk AEM. Neenan TX. Reedijk J. *J. Chem. Soc., Dalton Trans.* **1997**, 4561−4570. (c) Boelrijk, A. E. M.; van Velzen, M. M.; Neenan, T. X.; Reedijk, J.; Kooijman, H.; Spek, A. L. *J. Chem. Soc., Chem. Commun.* **1995**, 2465−2467. (d) Ley, S. V.; Norman, J.; Griffith, W. P.; Marsden, S. P. *Synthesis* **1994**, 639−666. (e) Murahashi, S.-I.; Naota, T. *Synthesis* **1993**, 433−440. (f) Morris, P. E.; Kiely, D. E. *J. Org. Chem.* **1987**, *52*, 1149−1152. (g) Griffith, W. P.; Ley, S. V.; Whitcombe, G. P.; White, A. D. *J. Chem. Soc., Chem. Commun.* **1987**, 1625−1627. (h) Gagne, R. R.; Marks, D. N. *Inorg. Chem.* **1984**, *23*, 65−74. (i) Sharpless, K. B.; Akashi, K.; Oshima, K. *Tetrahedron Lett.* **1976**, *29*, 2503−2506.

(3) Muller, J. G.; Acquaye, J. H.; Takeuchi, K. J. *Inorg. Chem.* **1992**, *31*, 4552−4557.

(4) Roecker, L.; Meyer, T. J. *J. Am. Chem. Soc.* **1987**, *109*, 746−754.

(5) Lee, D. G.; Van Den Engh, M. *Can. J. Chem.* **1972**, *50*, 2000−2009.

(6) Kochi, J. K. *Organometallic Mechanisms and Catalysis*; Academic Press: New York, 1978; pp 106−113 and references therein.

(7) Bernard, K. A.; Rees, W. M.; Atwood, J. D. *Organometallics* **1986**, *5*, 390−391.

(8) (a) Rankin, K. N.; Liu, Q.; Hendry, J.; Yee, H.; Noureldin, N. A.; Lee, D. G. *Tetrahedron Lett.* **1998**, *39*, 1095−1098. (b) Cheng, W. C.; Yu, W. Y.; Li, C. K.; Che, C. M. *J. Org. Chem.* **1995**, *60*, 6840−6846. (c) Lee, D. G.; Van Den Engh, M. *Can. J. Chem.* **1972**, *50*, 3129−3134.

(9) Lorber, C. Y.; Pauls, I.; Osborn, J. A. *Bull. Soc. Chim. Fr.* **1996**, *133*, 755−758.

(10) Scott, S. L.; Bakac, A.; Espenson, J. H. *J. Am. Chem Soc.* **1992**, *114*, 4205−4213.

(11) (a) Markó, I. E.; Giles, P. R.; Tsukazaki, M.; Brown, S. M.; Urch, C. J. *Science* **1996**, *274*, 2044−2046. (b) Bäckvall, J.-E.; Chowdhury, R. L.; Karlsson, U. *J. Chem. Soc., Chem. Commun.* **1991**, 473−475. (c) Bilgrien, C.; Davis, S.; Drago, R. S. *J. Am. Chem. Soc.* **1987**, *109*, 3786−3787. (d) Matsumoto, M.; Watanabe, N. *J. Org. Chem.* **1984**, *49*, 3435−3437. (e) Tang, R.; Diamond, S. E.; Neary, N.; Mares, F. *J. Chem. Soc., Chem. Commun.* **1978**, 562. (f) Neumann, R.; Dahan, M. *Nature* **1997**, *388*, 353−355. (g) Prati, L.; Rossi, M. *J. Mol. Catal. A* **1996**, *110*, 221−226.

(12) Markó, I. E.; Giles, P. R.; Tsukazaki, M.; Chellé-Regnaut, I.; Urch, C. J.; Brown, S. M. *J. Am. Chem. Soc.* **1997**, *119*, 12661−12662.

10.1021/ja982171y CCC: $19.00 © 2000 American Chemical Society
Published on Web 01/27/2000

Scheme 1

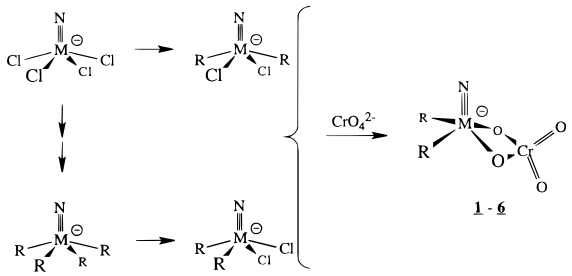

CrO_2] and [N(*n*-Bu)$_4$][Os(N)(CH$_3$)$_2$(μ-O)$_2$CrO$_2$] catalyze the selective oxidation of alcohols with molecular oxygen.[15] We also showed that one of these complexes reacts with dppe and catalyzes the oxidation of this phosphine with O_2.[16] In this report, we present a complete study on the oxidation of alcohols by [N(*n*-Bu)$_4$][Os(N)(CH$_2$SiMe$_3$)$_2$(μ-O)$_2$CrO$_2$] and related heterobimetallic complexes.

Results

Syntheses of Os−Cr and Ru−Cr Complexes. The reactions of the anionic osmium(VI) and ruthenium(VI) complexes [Os(N)(H$_2$SiMe$_3$)$_2$Cl$_2$]$^-$, [Os(N)Me$_2$Cl$_2$]$^-$, [Os(N)Me(CH$_2$SiMe$_3$)Cl$_2$]$^-$, [Ru(N)Me$_2$Cl$_2$]$^-$, and [Os(N)Ph$_2$Cl$_2$]$^-$ with aqueous potassium chromate produce stable organometallic complexes containing a bidentate chromate group. Alternatively, these osmium and ruthenium complexes react with silver chromate in dry CH_2Cl_2 solution to produce the chromate complexes (Scheme 1). These reactions with silver chromate require light and do not proceed when the reaction vessel is wrapped in aluminum foil.

In a typical preparation, we combined [N(*n*-Bu)$_4$][Os(N)(CH$_2$SiMe$_3$)$_2$Cl$_2$] and excess Ag_2CrO_4 in CH_2Cl_2 and stirred them for 12 h at room temperature under a UV lamp. The color of the solution changed from orange to dark purple over this time. Filtration removed the AgCl and unreacted Ag_2CrO_4. The product, [N(*n*-Bu)$_4$][Os(N)(CH$_2$SiMe$_3$)$_2$(μ-O)$_2$CrO$_2$] (**1a**), crystallized from hexane/methylene chloride solution in 94% yield. Crystals melted sharply at 119 °C without decomposition. The reaction between [N(*n*-Bu)$_4$][Os(N)(CH$_2$SiMe$_3$)$_2$Cl$_2$] in CH_2Cl_2 and K_2CrO_4 in water also gave **1a**, but the yield and purity of product were lower.

The ^{1}H and ^{13}C NMR spectra of **1a** show resonances associated with the alkylammonium cation and the alkyl groups. The two (trimethylsilyl)methyl ligands are equivalent with diastereotopic methylene protons. The shape of the resonance for the α protons is strongly solvent dependent. The four protons appear to be a singlet at 2.08 ppm in CD_2Cl_2 but are closely spaced doublets (J_{HH} = 7.1 Hz) at 2.09 and 2.17 ppm in $CDCl_3$ solution. The IR spectrum shows a medium-intensity sharp band for the osmium−nitride stretching vibration at 1111 cm^{-1}, very similar to the observations for other five-coordinate alkylosmium nitrido complexes.[17] The chromate group is clearly a bidentate ligand of the osmium with two strong, sharp bands at 948 and 928 cm^{-1} for the Cr−O asymmetric and symmetric stretching vibrations for the two terminal oxides. This is similar to the observations for other bidentate metal complexes of chromate.[18] The bridging Os−O−Cr stretching vibration should occur close to 800 cm^{-1}, but it is obscured by stronger bands associated with the alkyl ligands. The purple color of the complex is due to an intense visible absorption band at 504 nm.

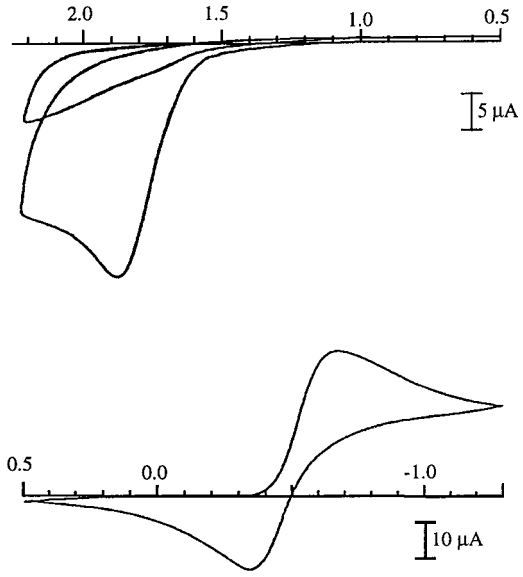

Figure 1. Cyclic voltammogram of **1**, volts vs Ag/AgCl.

The cyclic voltammogram of **1a** in CH_2Cl_2 shows the E_p of an irreversible oxidation wave at +1.88 V and the $E_{1/2}$ of a quasi-reversible reduction wave at −0.50 V vs Ag/AgCl (Figure 1). The irreversible oxidation is superimposed on background (0.1 M [N(*n*-Bu)$_4$][BF$_4$] in CH_2Cl_2) at the top of Figure 1. Controlled potential electrolysis indicates that each of these waves is associated with a one-electron process. The reduction is quasi-reversible with approximately equal anodic and cathodic currents and a peak-to-peak separation of 329 mV at a scan rate of 100 mV/s. The ΔE_p increases as the scan rate is increased. The reduction appears to be diffusion-controlled as indicated by the linearity of the plot of i_p vs $\nu^{1/2}$ over the range 50−2000 mV/s.

The tetraphenylphosphonium salt of the chromate complex, [PPh$_4$][Os(N)(CH$_2$SiMe$_3$)$_2$(μ-O)$_2$CrO$_2$] (**1b**), results from the reaction of [PPh$_4$][Os(N)(CH$_2$SiMe$_3$)$_2$Cl$_2$] and Ag_2CrO_4 or K_2CrO_4. The solubility of **1b** is lower than that of **1a** in organic solvents, and this complex is more difficult to crystallize, but the other physical properties and spectroscopic data are very similar or identical to those of **1a**.

The reaction of [N(*n*-Bu)$_4$][Ru(N)(CH$_2$SiMe$_3$)$_2$Cl$_2$] and Ag_2CrO_4 produced [N(*n*-Bu)$_4$][Ru(N)(CH$_2$SiMe$_3$)$_2$(μ-O)$_2$CrO$_2$] (**2**) in 54% yield. The ^{1}H and ^{13}C NMR spectra of **1a** and **2** are very similar. The ruthenium complex is dark orange rather than purple in solution because it lacks the visible absorption band found in **1**. The terminal Cr−O stretching vibrations shift by only 4 cm^{-1} from the position of those bands in **1**. The

(13) (a) Sterenberg, B. T.; McDonald, R.; Cowie, M. *Organometallics* **1997**, *16*, 2297−2312. (b) Mantovani, L.; Ceccon, A.; Gambaro, A.; Santi, S.; Ganis, P. *Organometallics* **1997**, *16*, 2682−2690. (c) Desmurs, P.; Visseaux, M.; Baudry, D.; Dormond, A.; Nief, F.; Ricard, F. *Organometallics* **1996**, *15*, 4178−4181. (d) Aubart, M. A.; Bergman, R. G *J. Am. Chem. Soc.* **1996**, *118*, 1793−1794. (e) Askham, F. R.; Carroll, K. M.; Briggs, P. M.; Rheingold, A. L.; Haggerty, B. S. *Organometallics* **1994**, *13*, 2139−2140. (f) Butts, M. D.; Bergman, R. G. *Organometallics* **1994**, *13*, 2668−2676. (g) *New Frontiers in Catalysis*; Guczi, L., Solymosi, F., Tétényi, P., Eds.; Elsevier Science Publishers: Amsterdam, 1993; Vol. 75, Part C. (h) Fraser, C.; Johnston, L.; Rheingold, A. L.; Haggerty, B. S.; Williams, G. K.; Whelan, J.; Bosnich, B. *Inorg. Chem.* **1992**, *31*, 1835−1844. (i) Stephan, D W. *Coord. Chem. Rev.* **1989**, *95*, 41−107.

(14) Lippard, S. J.; Berg, J. M. *Principles of Bioinorganic Chemistry*; University Science Books: Mill Valley, CA, 1994; Chapter 11.

(15) Zhang, N.; Mann, C.; Shapley, P. A. *J. Am. Chem. Soc.* **1988**, *110*, 6591−6592.

(16) Allen, J. L.; Shapley, P. A.; Wilson, S. R. *Organometallics* **1994**, *13*, 3749−3751.

(17) Marshman, R. W.; Shapley, P. A. *J. Am. Chem. Soc.* **1990**, *112*, 8369−8378.

(18) Coomber, R.; Griffith, W. P. *J. Chem. Soc. (A)* **1968**, 1128−1131.

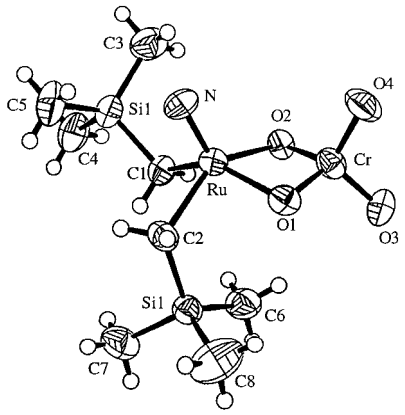

Figure 2. ORTEP diagram of $[Ru(N)(CH_2SiMe_3)_2(\mu\text{-}O)_2CrO_2]^-$.

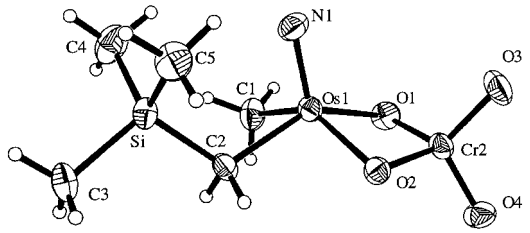

Figure 3. ORTEP diagram of $[Os(N)Me(CH_2SiMe_3)(\mu\text{-}O)_2CrO_2]^-$.

ruthenium−nitride stretching vibration is at 1082 cm^{-1} in the IR spectrum.

We prepared $[PPh_4][Os(N)(CH_3)_2(\mu\text{-}O)_2CrO_2]$ (**3**) from $[PPh_4][Os(N)(CH_3)_2Cl_2]$, $[PPh_4][Ru(N)(CH_3)_2(\mu\text{-}O)_2CrO_2]$ (**4**) from $[PPh_4][Ru(N)(CH_3)_2Cl_2]$, and $[N(n\text{-}Bu)_4][Os(N)Ph_2(\mu\text{-}O)_2CrO_2]$ (**5**) from $[N(n\text{-}Bu)_4][Os(N)Ph_2Cl_2]$. The chromate anion substituted for the chloride ligands in racemic $[PPh_4][Os(N)Me(CH_2SiMe_3)Cl_2]$ and produced both enantiomers of the chiral Os−Cr complex, $[PPh_4][Os(N)Me(CH_2SiMe_3)(\mu\text{-}O)_2CrO_2]$ (**6**). The IR spectra of each of these complexes clearly indicate the presence of a terminal nitride and bidentate chromate group.

Molecular Structures of 2 and 6. We determined the molecular structures of **2** and **6** by single-crystal X-ray diffraction. For each salt, the anion and cation are well separated. A molecule of CH_2Cl_2 crystallized with **6**. Figure 2 shows a view of $[Ru(N)(CH_2SiMe_3)_2(\mu\text{-}O)_2CrO_2]^-$, and one of the two enantiomers of $[Os(N)Me(CH_2SiMe_3)(\mu\text{-}O)_2CrO_2]^-$ is shown in Figure 3. Table 1 includes selected bond distances and angles of both complexes.

The ruthenium center in **2** has a distorted square pyramidal geometry with the nitrido ligand in the apical position. The ruthenium atom is above the plane of the four basal ligands. This is common in five-coordinate nitridoruthenium complexes. The nitrogen−ruthenium−oxygen angles are greater than the nitrogen−ruthenium−carbon angles, probably due to repulsion between lone pairs on the nitride and the bridging oxides. The ruthenium−nitrogen distance and the average ruthenium−carbon distance in **2** are 1.612(7) and 2.099 Å, respectively. The ruthenium−nitrogen distance is longer than the Ru−N distances of 1.570(7) Å in $[Ph_4As][Ru(N)Cl_4]$ and 1.580(1) Å in $[N(n\text{-}Bu)_4][Ru(N)(CH_3)_4]$.[19,20] Presumably, the steric requirements imposed by the (trimethylsilyl)methyl ligand are responsible for the increase in this bond length.[21] The average terminal Cr=O distance is 1.603 Å, while the average bridging Cr−O distance is 1.725 Å. These Cr−O bond lengths are longer than the bond distances found in $[L_2Fe_2(\mu\text{-}CrO_4)_3]\cdot H_2O$ (1.678, 1.574 Å).[22] The ruthenium−chromium distance is 2.617(2) Å.

Table 1. Selected Bond Distances and Angles for **2** and **6**

2		**6**	
Distances, Å			
Ru−Cr	2.617(2)	Os−Cr	2.5627(1)
Ru−O1	2.061(6)	Os−O1	1.996(5)
Ru−O2	2.049(5)	Os−O2	2.017(4)
Ru−N1	1.612(7)	Os−N1	1.650(6)
Ru−C1	2.099(9)	Os−C1	2.085(8)
Ru−C2	2.098(8)	Os−C2	2.091(6)
Cr−O1	1.722(6)	Cr−O1	1.746(5)
Cr−O2	1.728(6)	Cr−O2	1.756(4)
Cr−O3	1.604(7)	Cr−O3	1.587(5)
Cr−O4	1.602(6)	Cr−O4	1.603(5)
Angles, deg			
N−Ru−C1	101.8(4)	N−Os−C1	101.8(3)
N−Ru−C2	102.6(4)	N−Os−C2	101.5(3)
O1−Ru−N	113.9(3)	O1−Os−N	114.4(3)
O2−Ru−N	117.1(3)	O2−Os−N	116.4(3)
C1−Ru−C2	85.3(3)	C1−Os−C2	84.6(3)
O1−Ru−O2	81.0(2)	O1−Os−O2	84.2(2)
O1−Cr−O2	101.4(3)	O1−Cr−O2	100.4(2)
O3−Cr−O4	110.8(4)	O3−Cr−O4	111.3(3)
O1−Cr−O4	111.6(3)	O1−Cr−O4	109.4(3)
O1−Cr−O3	111.6(3)	O1−Cr−O3	113.7(3)
Cr−O1−Ru	87.0(2)	Cr−O1−Os	86.2(2)
Cr−O2−Ru	87.3(2)	Cr−O2−Os	85.3(2)

Scheme 2

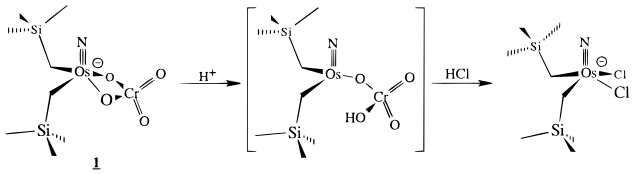

1

Complex **6** is structurally similar to **2**. The osmium center in **6** has a distorted square pyramidal geometry with the nitrido ligand in the apical position and the osmium atom above the plane of the four basal ligands. The nitrogen−osmium−oxygen angles are greater than the nitrogen−osmium−carbon angles by as much as 12°. The osmium−nitrogen distance of 1.650(6) Å is slightly longer than the Ru−N distance in **2** and longer than the Os−N distance in $[N(n\text{-}Bu)_4][Os(N)(CH_2SiMe_3)_4]$, 1.631(8) Å.[23] The osmium−chromium distance in **6** is shorter than the ruthenium−chromium distance in **2** by 0.05 Å, and the Cr−O-M angle is more acute in **6** than in **2**.

Reaction Chemistry of 1. The osmium chromate complex **1** is stable in the presence of triphenylphosphine, cyclohexene, carbon monoxide, ethers, ferrocene, and dimethyl sulfide. This is surprising because chromium(VI) oxides are active oxidizing agents. They are capable of oxidizing triaryl- and trialkylphosphines, dialkyl sulfides, alcohols, aldehydes, alkenes, and even some activated hydrocarbons.[1,24]

Acids and other electrophiles react rapidly with **1**. The addition of $HCl_{(g)}$ to a purple solution of **1a** at −78 °C causes the color to change to blue (Scheme 2). The absorption band at 504 nm broadens considerably with the addition of the acid.

(19) Shapley, P. A.; Kim, H. S.; Wilson, S. R. *Organometallics* **1988**, *7*, 928−933.
(20) Phillips, F. L.; Skapski, A. C. *Acta Crystallogr.* **1975**, *B31*, 2667−2670.
(21) Bright, D.; Ibers, J. A. *Inorg. Chem.* **1969**, *8*, 709.
(22) Chaudhuri, P.; Winter, M.; Wieghardt, K.; Gehring, S.; Haase, W.; Nuber, B.; Weiss, L. *Inorg. Chem.* **1988**, *27*, 1564.
(23) Belmonte, P. A.; Own, Z. Y. *J. Am. Chem. Soc.* **1984**, *106*, 7493−7496.
(24) (a) Piancatelli, G.; Scettri, A.; D′Auria, M. *Synthesis* **1982**, 245−258. (b) Collins, J. C.; Hess, W. W.; Frank, F. J. Tetrahedron Lett. **1968**, 3363−3366.

Scheme 3

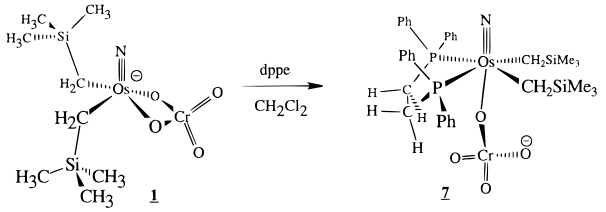

As the solution warms to room temperature, the initially formed complex decomposes and $[N(n\text{-}Bu)_4][Os(N)(CH_2SiMe_3)_2Cl_2]$ forms. The addition of $HBF_4{\cdot}OMe_2$ to **1** in toluene solution gives a blue solution with a visible spectrum identical to that of the protonated complex. Addition of an equivalent of $CH_3OSO_2CF_3$ to **1** also gives a blue product. The methylation product, presumably $[Os(N)(CH_2SiMe_3)_2(\mu\text{-}O)CrO_2(OCH_3)]$, is stable for hours at room temperature. Because it is highly soluble in hexane, we have not been able to isolate it in pure form. The product is paramagnetic, and its IR spectrum contains bands due to Os−N and terminal Cr−O stretching vibrations.

Methanol forms a complex with **1**. The resonances for the α protons of the alkyl groups in **1a** shift significantly in the ^1H NMR spectrum when methanol or methanol-d_3 is added to the solution. The osmium−nitrogen stretching vibration shifts to lower energy in the solution IR spectrum, but the energy of the terminal chromium−oxo stretches does not change. We see these changes in the IR and NMR spectra of **1** only in high concentrations of methanol. We do not observe adduct formation with bulkier alcohols.

The osmium chromate complexes react with bis(diphenylphosphino)ethane to give dppe complexes. The addition of dppe to either **1a** or **1b** produces $[N(n\text{-}Bu)_4][Os(N)(CH_2SiMe_3)_2(dppe)CrO_4]$ (**7a**) or $[PPh_4][Os(N)(CH_2SiMe_3)_2(dppe)CrO_4]$ (**7b**) (Scheme 3). They form analytically pure, yellow crystals from methylene chloride/hexane solutions. A single-crystal X-ray diffraction study of the molecular structure of **7b** shows that the dppe chelates the osmium center, which has a distorted octahedral geometry.[16] The chromate group is monodentate with a distorted tetrahedral geometry around the chromium center. Complex **1a** does not react with the arsenic analogue, $Ph_2AsCH_2CH_2AsPh_2$.

The anionic complex $[Os(N)(CH_2SiMe_3)_2(\mu\text{-}O)_2CrO_2]^-$ reacts with hydrogen peroxide. When **1b** is treated with a stoichiometric amount of 30% hydrogen peroxide in water, the color of the solution changes from purple to orange. The IR and ^1H NMR spectra indicate the presence of tetraphenylphosphonium cation and (trimethylsilyl)methyl ligands. In the IR spectrum, the terminal nitride is evident, but the chromium−oxo stretching vibrations are significantly modified. The complex is unstable, and it decomposes to **1b** and an insoluble brown material. The reaction between **1** and Na_2O_2 in water gives similar results. The reaction of **1** with excess 30% hydrogen peroxide in H_2O/CH_2Cl_2 gives an intensely colored blue product. The elemental analysis for this complex indicates an empirical formula of $[N(n\text{-}Bu)_4]_2[OsCrO_5]$.

Catalysis by 1 of Alcohol Oxidation in Air. Complex **1** oxidizes benzylic, primary, and secondary alcohols to the corresponding carbonyl compounds (Table 2). In air, these reactions are catalytic. Alcohol oxidation reactions are slow at room temperature, and the rate of the reaction depends on the steric bulk of the alcohol. In competition experiments, primary alcohols are always oxidized faster than secondary alcohols (Table 3). Oxidation of primary alcohols produces only aldehydes. There is no skeletal isomerization with the cyclopropyl-substituted alcohol. With unsaturated alcohols, there is no oxidation of the double bond and no isomerization. The rate of oxidation of all the *para*-substituted benzyl alcohols ($p\text{-}XC_6H_4CH_2OH$; X = Cl, H, CH_3, OCH_3) by **1a** in air is the same within experimental error. *p*-Nitrobenzyl alcohol reacts irreversibly with the catalyst.

Table 2. Catalytic Oxidation of Alcohols by **1a**

Substrate	Product	TO[a]
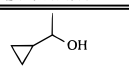	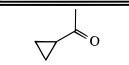	2
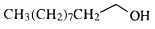	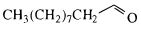	6
	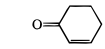	7
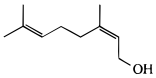	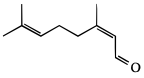	9
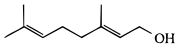	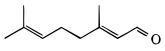	13
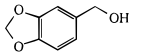	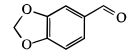	15
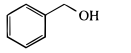	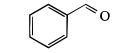	19
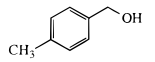	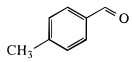	19
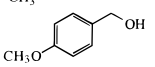	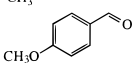	19
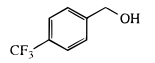	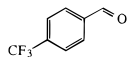	19
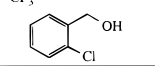	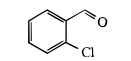	19

[a] Reactions were run with a 20/1 ratio of alcohol to catalyst in toluene at 70 °C, and turnovers (TO) were measured after 3 h.

Table 3. Competition between Oxidation of Primary and Secondary Alcohols by **1a**[a]

Substrates	Aldehyde/Ketone
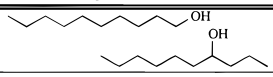	14
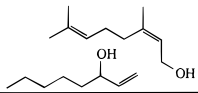	10
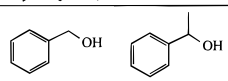	4

Scheme 4

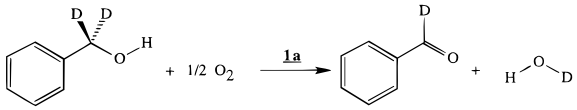

We investigated the stoichiometry of benzyl alcohol oxidation to benzaldehyde by ^2H NMR spectroscopy. The reaction of **1a** and $C_6H_5CD_2OH$ in C_6H_6 at 60 °C in the probe of the NMR spectrometer produced water (HDO, D_2O, H_2O) and C_6H_6CDO in a 1:1 ratio (Scheme 4). When **1a** reacted with $C_6H_5CH(D)OH$, a mixture of C_6H_5CHO and C_6H_5CDO formed in a 1:1.9 ratio.

When O_2 was insufficient, the reaction between **1** and benzyl alcohol produced a green, paramagnetic organometallic product (**8**), along with benzaldehyde and water. The ESR spectrum of

Scheme 5

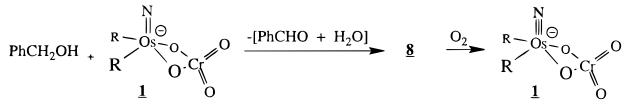

8 at room temperature showed two resonances at $g = 3.3842$, 1.9803. The spectrum is quite different from that of either Cr(IV) or Os(IV) and may contain Os(V) and Cr(V) centers.[25] The UV−visible spectrum showed a weak, broad absorption centered at 560 nm. The IR spectrum includes two very strong bands at 954, 832 cm^{-1} which can be assigned to the terminal Cr−O stretching vibrations. Complex **8** is thermally unstable, but it reacts with molecular oxygen to form **1** (Scheme 5).

When **1** reacted with benzyl alcohol under $^{17}O_2$, the recovered catalyst contained labeled oxygen in the bridging but not the terminal oxo positions. The ^{17}O NMR spectrum of the recrystallized, recovered **1** contained a single resonance in the bridging metal oxide region at 537 ppm.[26] The IR spectrum showed no shift in the positions of the terminal Cr═O stretching vibrations. In a separate experiment, we followed the stoichiometric reaction between benzyl alcohol, $^{17}O_2$, and **1a** by ^1H and ^{17}O NMR spectroscopy. The water initially produced in the reaction contained no labeled oxygen, but there was some ^{17}O substitution in the bridging oxo position. After additional benzyl alcohol and $^{17}O_2$ were added to the reaction mixture, ^{17}O-labeled water was produced.

All of the bimetallic complexes **1**−**6** oxidize alcohols in a similar manner. We obtained rate data under various conditions for the oxidation of benzyl alcohol by **1a** and **5**, but we obtained rate data for benzyl alcohol oxidation only under a single set of conditions for **2** and **4**. The oxidation of benzyl alcohol is first order in catalyst and first order in alcohol. For reactions in toluene at 70 °C, the reaction rate constant decreases: **2** (3.8×10^{-1} M^{-1} s^{-1}) > **5** (5.4×10^{-2} M^{-1} s^{-1}) > **1** (2.9×10^{-2} M^{-1} s^{-1}). The rate for the other ruthenium−chromium catalyst, **4**, is intermediate between those of **2** and **5** with a second-order rate constant of 6.3×10^{-2} M^{-1} s^{-1}. However, the solvent for oxidation reactions with **4** was CH_3NO_2 because of the insolubility of **4** in toluene, and this certainly affects the rate. These catalyzed oxidation reactions are faster in solvents of low dielectric constant. Toluene is a better solvent for these reactions than acetonitrile or nitromethane (Figure 4).

The dependence of the reaction rate on O_2 concentration is more complex. At low partial pressure of O_2, the rate is directly proportional to O_2 partial pressure (Figure 5). At high concentrations of O_2, there is an inverse dependence of the partial pressure on the rate constant.

The activation parameters were calculated from the dependence of the rate contant with temperature. For the oxidation of benzyl alcohol by **1** in air at 1 atm pressure in C_6D_6 solution, $\Delta H^{\ddagger}$ was 10.6 kcal/mol and $\Delta S^{\ddagger}$ was −34 eu.

Comparison of 1a and 5 in the Oxidation of Alcohols. Complex **5** is similar to **1** in the oxidation of alcohols. The rate of reaction of benzyl alcohol with molecular oxygen catalyzed by **5** is first order in alcohol and first order in catalyst concentration, with a second-order rate constant of 5.4×10^{-2} M^{-1} s^{-1} at 65 °C. As with **1**, the oxidation reaction is faster in solvents of low polarity than in more polar solvents. Benzylic alcohols are oxidized at a higher rate than primary alcohols, and primary alcohols are oxidized faster than secondary alcohols. There is no reaction between **5** and alkenes, pyridine, or PPh_3. In contrast to **1**, in the oxidation of geraniol catalyzed by **5**, there is some isomerization of the C−C double bond, and both geranial and neral are formed.

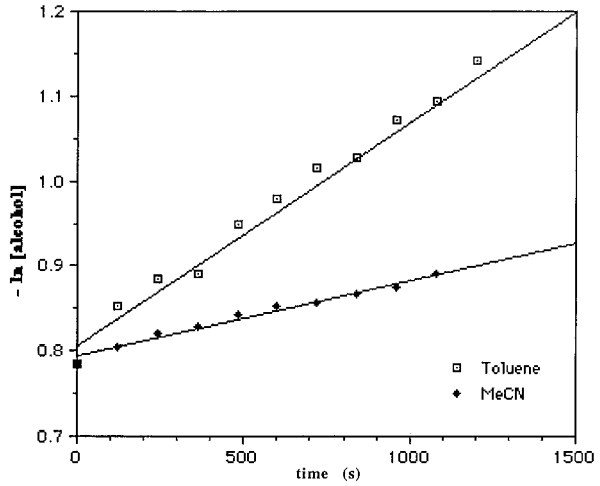

Figure 4. Plots of −ln [$PhCH_2OH$] vs time (seconds) for the oxidation reaction catalyzed by **1** in toluene-d_8 and acetonitrile-d_3.

In studying the reactivity of **5**, we observed that this complex reduces benzaldehyde to benzyl alcohol in the presence of water. The oxidation of benzyl alcohol catalyzed by **5** is a reversible reaction (Scheme 6).

Catalytic Oxidation of dppe by 1. Although **1** does not react with PPh_3 even at elevated temperatures, it does react with more basic phosphines and can function as a phosphine oxidation catalyst. Complex **1** reacts with dppe to produce a product (**7**) in which the phosphine ligand is bidentate and the chromate ligand is monodentate. Yellow solutions of **7a** are air sensitive and decompose over a period of several days at room temperature to give a purple solution consisting of **1a** and $Ph_2P(O)CH_2$-$CH_2P(O)Ph_2$ (Scheme 7, R = CH_2SiMe_3). In the presence of excess dppe, the reaction is catalytic.

The related osmium complexes $[N(n\text{-}Bu)_4][Os(N)(CH_2SiMe_3)_2$-$(SO_4)]$ and $[N(n\text{-}Bu)_4][Os(N)(CH_2SiMe_3)_2(CO_3)]$ react with dppe and O_2 at 60−70 °C in toluene to give a 20−30% yield of $Ph_2P(O)CH_2CH_2P(O)Ph_2$, but the oxidations are not catalytic. The dppe complex $[Os(N)(CH_2SiMe_3)_2(dppe)(NCMe)][BF_4]$ decomposes in the presence of O_2 under these conditions to give a small amount of phosphine oxide and a black, insoluble solid. The quantity of the phosphine oxide is not increased when the decomposition reaction is carried out in the presence of excess dppe or chromate ion. A similar complex prepared in the absence of acetonitrile, $[Os(N)(CH_2SiMe_3)_2(dppe)][BF_4]$, does not form the phosphine oxide when exposed to air, even in the presence of excess dppe. We prepared a monometallic complex very similar to **7** by the reaction of $[N(n\text{-}Bu)_4][Os$-$(N)(CH_2SiMe_3)_2(SO_4)]$ with dppe. There is no reaction between either $Os(N)(CH_2SiMe_3)_2(dppe)Cl$ or $Os(N)(CH_2SiMe_3)_2(dppe)$-$(OSO_3)$ and O_2.

Kinetic Studies of the Catalytic Oxidation of dppe by 1. Complex **1** catalyzes the oxidation of dppe by O_2 in toluene solution under air at 60 °C with a turnover number of 13 per hour. More than 40 equiv of dppe per equivalent of catalyst **1**

(25) (a) Wertz, J. E.; Bolton, J. R. *Electron Spin Resonance*; Chapman and Hall: New York, 1986; Chapter 10. (b) Abragam, A.; Bleaney, B. *Electron Paramagnetic Resonance of Transition Ions*; Dover Publications: New York, 1986; p 480. (c) Hoskins, R. H.; Soffer, B. H. *Phys Rev.* **1964,** *133A*, 490.

(26) (a) Kintzinger, J. P. *Oxygen-17 and Silicon-29*; Springer-Verlag: New York, 1981; pp 33−34. (b) Rodger, C.; Sheppard, N.; Mcfarlane, C.; Mcfarlane, W. *NMR and the Periodic Table*; Academic Press: New York, 1978; pp 383−400. (c) Figgis, B. N.; Kidd, R. G.; Nyholm, R. S. *Can. J. Chem.* **1965**, *43*, 145−153. (d) Jackson, J. A.; Taube, H. *J. Phys. Chem.* **1965**, *69*, 1844−1849.

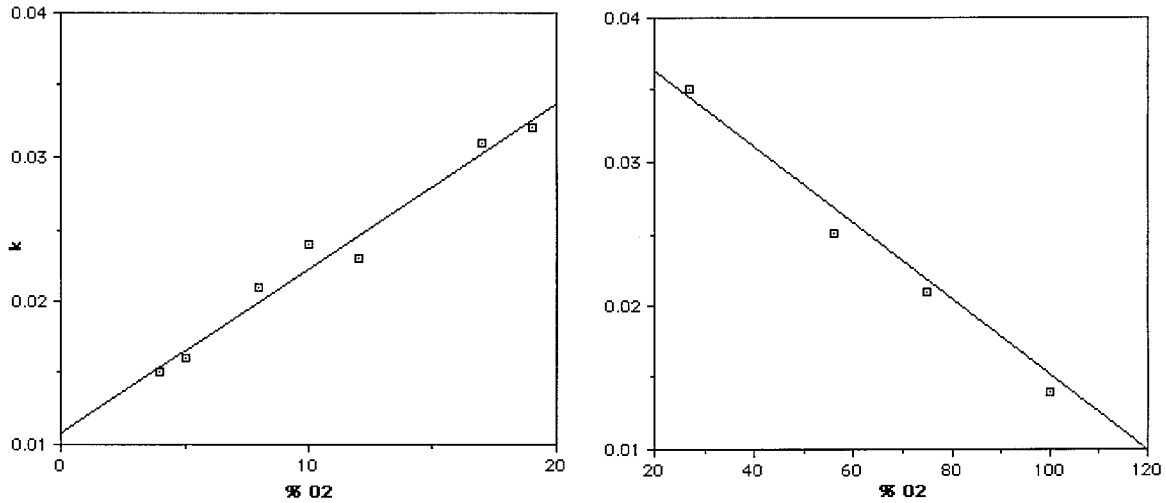

Figure 5. Plots of second-order rate constants k (M^{-1} s^{-1}) vs % O_2 in an O_2/N_2 gas mixture.

Scheme 6

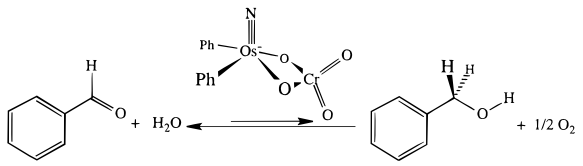

Scheme 7

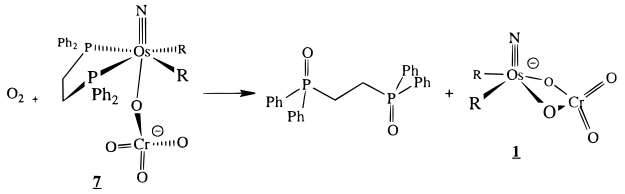

is oxidized without loss of catalytic activity. Under identical conditions in the absence of **1**, there is no measurable oxidation of dppe. Meyer and Dovletoglou[27] reported that the reduction of ruthenium and osmium oxides by dppe produces the mono-oxide $Ph_2P(O)CH_2CH_2PPh_2$, but none of this mono-oxide results from the oxidation with **1**. The oxidation of dppe by **1** in air was second order (first order in **1** and in dppe), with $\Delta H^{\ddagger} = 15.2$ kcal/mol and $\Delta S^{\ddagger} = -12$ eu.

Oxygen Labeling Studies of the Catalytic Oxidation of dppe by 1. When a solution of **7** in toluene reacted with $^{18}O_2$ (95% isotopic purity) under stoichiometric conditions, the products were **1**, 0.5 equiv of dppe, and 0.5 equiv of $Ph_2P(O)CH_2CH_2P(O)Ph_2$. An EI mass spectrum showed that the $Ph_2P(O)CH_2CH_2P(O)Ph_2$ in the product mixture contained 91.8% unlabeled phosphine oxide, 6.7% with a single ^{18}O label, and 1.5% with two ^{18}O atoms per molecule. Under catalytic conditions, **7** reacted with dppe and $^{18}O_2/^{16}O_2$ (24% $^{18}O_2$ in $^{16}O_2$) to give $Ph_2P(O)CH_2CH_2P(O)Ph_2$ with a statistical amount of ^{18}O.

Discussion

Five-coordinate osmium and ruthenium complexes, such as $[N(n\text{-}Bu)_4][Os(N)(CH_2SiMe_3)_2Cl_2]$, weakly coordinate donors trans to the nitride ligand.[28] Substitution of the two chloride ligands for a chromate dianion probably goes through an associative pathway. Carbonate and sulfate are better ligands for osmium(VI) than is chromate, and these dianions substitute for chloride ligands much more rapidly than does chromate.[29] Silver chromate reacts more rapidly than potassium chromate with $[N(n\text{-}Bu)_4][Os(N)(CH_2SiMe_3)_2Cl_2]$ and related dihalides because the silver chloride product is insoluble and a back reaction is not possible.

Electrochemical studies of **1a** show that the chromate is not a strong σ donor ligand. Changing ligands on the osmium(VI) center changes the electron density of the metal and its oxidation potential. The oxidation potential in the series of complexes $[N(n\text{-}Bu)_4]$ $[Os(N)Cl_{4-n}(CH_2SiMe_3)_n]$ ($n = 0, 2, 4$) decreases significantly with the substitution of electron-withdrawing chloride ligands for electron-donating alkyl groups. The oxidation potentials decrease from 2.12 V for $[N(n\text{-}Bu)_4][Os(N)Cl_4]$ to 1.05 V for *trans*-$[N(n\text{-}Bu)_4][Os(N)(CH_2SiMe_3)_2Cl_2]$ to 0.64 V for $[N(n\text{-}Bu)_4][Os(N)(CH_2SiMe_3)_4]$.[17] The osmium atom in $[N(n\text{-}Bu)_4][Os(N)(CH_2SiMe_3)_2(\mu\text{-}O)_2CrO_2]$ (**1a**) has an oxidation wave at +1.88 V and is more electron-poor than *trans*-$[N(n\text{-}Bu)_4][Os(N)(CH_2SiMe_3)_2Cl_2]$.

Structural studies of **2** and **6** show a significant interaction between the chromate ligand and the π orbitals of the terminal nitride ligand on each complex. Nitridoosmium(VI) and nitridoruthenium(VI) distort from the square pyramidal geometry (increasing the nitrido-basal ligand angle) due to interactions between lone pairs on the basal ligand and the nitrido π orbital or due to steric interactions.[20,23,30] In both **2** and **6**, the N−M−O angles are greater than the N−M−C angles. Because the chromate ligand is less sterically demanding than the alkyl ligands on these complexes, the distortion must be due to electronic repulsion. The nitrido−metal bond distances in these two complexes are significantly longer than those in all related nitridoruthenium(VI) and nitridoosmium(VI) complexes, indicating that the repulsion between electrons on the bridging oxo groups and electrons in the nitrido−metal π orbitals weakens the M−N bond.

Both metal centers in **1** are coordinatively unsaturated. The chromium is formally a Cr(VI), four-coordinate, 12-electron center, and the osmium is an Os(VI), five-coordinate, 16-electron center. Given the lower number of electrons on the chromium, it would be reasonable to assume that Lewis bases would coordinate to it in preference to the more electron-rich osmium. Interestingly, donors coordinate to the osmium center, not the

(27) Dovletoglou, A.; Meyer, T. J. *J. Am. Chem. Soc.* **1994**, *116*, 215−223.

(28) Shapley, P. A.; Marshman, R. R.; Shusta, J. M.; Gebeyehu, Z.; Wilson, S. R. *Inorg. Chem.* **1994**, *33*, 498−502.

(29) Zhang, N.; Shapley, P. A. *Inorg. Chem.* **1988**, *27*, 976−977.

(30) Nugent, W. A.; Mayer, J. M. *Metal−Ligand Multiple Bonds*; John Wiley & Sons: New York, 1988; Chapter 4.

chromium center in **1**. The bidentate donor dppe coordinates to the osmium center when it forms **7**. There is no evidence for dppe coordination to Cr in solution or in the solid state.

Methanol coordinates weakly to the Os(VI) atom in solution. This is clear from the lowering of the energy of the Os−N stretching vibration, consistent with coordination of a donor molecule trans to the nitride.[17,30] We see no shift to lower energy of the Cr−O stretching bands as would be expected if the alcohol coordinated and donated electron density to the chromium atom. The equilibrium between $[Os(N)(HOCH_3)(CH_2SiMe_3)_2(CrO_4)]^-$ and $[Os(N)(CH_2SiMe_3)_2(CrO_4)]^-$ favors the five-coordinate osmium complex, and we are able to observe the methanol adduct only in high concentrations of methanol. We can readily observe complex formation with methanol because this alcohol is only slowly oxidized by **1**. We assume that other alcohols also reversibly coordinate to this site on osmium prior to oxidation. Although the initial step in oxidation of alcohols by chromate salts and related species involves interaction of the alcohol with chromium(VI) and formation of a chromium alkoxide complex,[31] the first step in alcohol oxidation by **1** is probably coordination of the alcohol to osmium.

Acid reacts with **1** to generate an unstable, paramagnetic complex, and methylation with $MeOSO_2CF_3$ gives a similar but more stable complex. There are three basic sites in the molecule: the terminal nitride and the two bridging oxo groups. The terminal chromium oxo groups are electrophilic,[32] like electrophilic terminal oxides in other metal oxo complexes,[33] and are not likely to be protonated by acid. The nitride ligand in $[NOs(CH_2SiMe_3)_4]^-$ does not reversibly add a proton but is probably involved in the protonolysis of $Os-CH_2SiMe_3$ bonds with strong acid.[17] Electrophilic attack on **1** by methyl trifluoromethanesulfonate gives a stable, diamagnetic methylimido complex.[34] In the IR spectra of the protonation and methylation products derived from **1**, the Os−N stretching vibration of the terminal nitride remains intact, and there is no evidence of Os−NH or Os−NMe groups. Protonation or methylation of **1** probably gives $[Os(N)(CH_2SiMe_3)_2(OCrO_2OH)]$ or $[Os(N)(CH_2SiMe_3)_2(OCrO_2OCH_3)]$, respectively.

Decomposition of $[Os(N)(CH_2SiMe_3)_2(OCrO_2OH)]$ in the absence of a donor, such as chloride, probably results from loss of alkane. This is common in the chemistry of osmium(VI) alkyl complexes. The protonated product is more likely to lose Me_4Si than the methylated product is to lose $Me_3SiCH_2CH_3$, so the methylated product is more thermally stable. In the presence of Cl^-, chloride adds to the unsaturated intermediate, and the oxyanion is displaced. The dialkyldichloro complex $[Os(N)Cl_2(CH_2SiMe_3)_2]^-$ is stable to acid.[17]

The protonated and alkylated products are paramagnetic, indicating trigonal pyramidal rather than square pyramidal geometry of the osmium center. In all of these complexes, the Cr centers have a d^0 electron configuration and the Os centers d^2. Square pyramidal **1** is diamagnetic because the HOMO, the d_{xy} orbital, is well separated in energy from the empty $d_{x^2-y^2}$ orbital.[35] Electrophilic addition to a bridging oxo, giving $(N)(Me_3SiCH_2)_2Os(\mu\text{-}O)(\mu\text{-}OE)CrO_2$ (where E = H, CH_3), does not change the geometry around the osmium, and this compound should also be diamagnetic. Dissociation of the hydroxo group would produce a distorted trigonal pyramidal complex, $(N)(Me_3SiCH_2)_2Os(\mu\text{-}O)CrO_2(OE)$. In this geometry, the d_{xy} and $d_{x^2-y^2}$ orbitals would be similar in energy, and occupation of both orbitals would give a paramagnetic complex.

The coordination of an alcohol molecule to osmium would increase the acidity of the hydroxy proton. Proton transfer from the coordinated alcohol RCH_2OH to one of the bridging oxo groups would give an alkoxide intermediate, $[(RCH_2O)(Me_3SiCH_2)_2(N)Os(\mu\text{-}O)CrO_2(OH)]^-$. The osmium center in this intermediate, unlike that in $(N)(Me_3SiCH_2)_2Os(\mu\text{-}O)CrO_2(OH)$, would be five-coordinate, square pyramidal, and diamagnetic.

The alkoxy group in $[(RCH_2O)(Me_3SiCH_2)_2(N)Os(\mu\text{-}O)CrO_2(OH)]^-$ is likely oxidized through a concerted β-hydrogen elimination mechanism. We can rule out hydride abstraction by a chromium oxo group because this would give a carbocation intermediate. In the oxidation of *para*-substituted benzyl alcohols, electron-donating substituents in the *para* position should accelerate the reaction by stabilizing the intermediate, and electron-withdrawing substitutents should decelerate it, but we observed no affect of the *para* substituent on the rate of the reaction.[36] A reaction that proceeds through hydrogen atom abstraction and formation of a radical intermediate should show the same type of electronic effect (although of a smaller magnitude) as the hydride abstraction mechanism. The lack of isomerization in the oxidation of *cis*- and *trans*-allylic alcohols, and oxidation of cyclopropylmethanol without ring-opening, also argue against a radical mechanism. The deuterium isotope effect on the rate of the reaction is in the range of those of other concerted β-hydrogen elimination reactions[37] and smaller than those typically observed in oxidation reactions with radical[10,38] or carbocation intermediates.[3,39]

We found that k_H/k_D was 1.9 in the oxidation of PhCHDOH. Use of this substrate (with both a hydrogen and a deuterium at the proto-carbonyl carbon) gives us an accurate intramolecular determination of the KIE. Isotope effects for the oxidation of benzyl alcohol by transition metal catalyts vary widely from small values on the order of ours to 50 (indicating quantum mechanical tunneling of the hydrogen). The value we see is quite small. This is expected for reactions in which the C−H(D)−X angle in the transition state is not linear.

Elimination of water from an $[(H)(Me_3SiCH_2)_2(N)Os(\mu\text{-}O)CrO_2(OH)]^-$ intermediate could produce **8**. Complex **8** is a thermally unstable, reactive intermediate in the reaction and is poorly characterized. A possible structure for **8** is given in Scheme 8. Binuclear reductive elimination reactions usually involve loss of a hydride on one metal along with another anionic ligand on the second metal and form a metal−metal bond. Both proton-transfer and hydrogen atom-transfer mechanisms have been proposed for these reactions.[40]

(31) Rocek, J.; Westheimer, F. H.; Eshenmoser, A.; Moldovanyi, L.; Schreiber, J. *Helv. Chim. Acta* **1962**, *45*, 2554.

(32) (a) Sharpless, K. B.; Teranishi, A. Y.; Bäckvall, J.-E. *J. Am. Chem. Soc.* **1977**, *99*, 3120−3128. (b) Samsel, E. G.; Srinivasan, K.; Kochi, J. K. *J. Am. Chem. Soc.* **1985**, *107*, 7606−7617.

(33) Dumez, D. D.; Mayer, J. M. *Inorg. Chem.* **1995**, *34*, 6396−6401.

(34) Shapley, P. A.; Own, Z. Y.; Huffman, J. C. *Organometallics* **1986**, *5*, 1269−1271.

(35) Cowman, C. D.; Trogler, W. C.; Mann, K. R.; Poon, C. K.; Gray, H. B. *Inorg. Chem.* **1976**, *15*, 1747−1751.

(36) Topsom, R. D. *Prog. Phys. Org. Chem.* **1976**, *12*, 1−20.

(37) The kinetic isotope effect on the decomposition of many metal alkyl complexes is in the range 1.4−2.3, but Boncella et al. found a deuterium isotope effect of 6.5 for a β hydrogen elimination in a tungsten complex. See: (a) Wang, S.-Y. S.; Abboud, K. A.; Boncella, J. M. *J. Am. Chem. Soc.* **1997**, *119*, 11990−11991. (b) Burger, B. J.; Thompson, M. E.; Cotter, W. D.; Bercaw, J. E. *J. Am. Chem. Soc.* **1990**, *112*, 1566−1577. (c) Whitesides, G. M. *Pure Appl. Chem.* **1981**, *53*, 287. (d) McCarthy, T. J.; Nuzzo, R. G.; Whitesides, G. M. *J. Am. Chem. Soc.* **1981**, *103*, 1676; 3396; 3404. (e) Ozawa, F.; Ito, T.; Yamamoto, A. *J. Am. Chem. Soc.* **1980**, *102*, 6457. (f) Ikariya, T.; Yamamoto, A. *J. Organomet. Chem.* **1976**, *120*, 257−284. (g) Evans, J.; Schwarts, J.; Urguhart, P. W. *J. Organomet. Chem.* **1974**, 81, C37−C39.

(38) Bockman, T. M.; Hubig, S. M.; Kochi, J. K. *J. Am. Chem. Soc.* **1998**, *120*, 2826−2830.

(39) (a) Che, C.-M.; Tang, W.-T.; Lee, W.-O.; Wong, K.-Y.; Lau, T.-C. *J. Chem. Soc., Dalton Trans.* **1992**, 1551−1556. (b) Roecker, L.; Meyer, T. J. *J. Am. Chem. Soc.* **1987**, *109*, 746−754.

Scheme 8. Proposed Catalytic Cycle for the Oxidation of Benzyl Alcohol by **1**

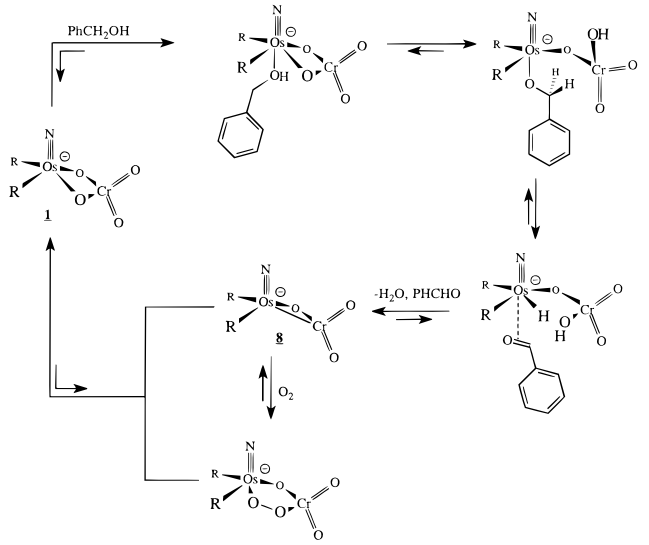

Molecular oxygen adds to the reactive Os−Cr bond in **8** and produces **1**. Initially, a μ-peroxide complex could be formed.[41] The peroxide complex could combine with an additional equivalent of **8** and transfer one of the peroxo oxygen atoms. This would explain why, when labeled O_2 adds to the complex, the labeled oxygens in the product bridge the two metals. At low partial pressures of O_2, the rate of the reaction depends directly on the concentration of O_2 because the rate-determining step under these conditions is the addition of oxygen to the Os−Cr bond. At high concentrations of O_2, the rate actually decreases with additional oxygen pressure. More of **8** converts to $[(Me_3SiCH_2)_2(N)Os(\mu\text{-}O)(\mu\text{-}O_2)CrO_2]^-$, and the concentration of **8** decreases. This reduces the rate of the oxygen atom-transfer step. Another possibility is that O_2 reacts reversibly with one of the intermediates to form a species outside the catalytic cycle so that under high oxygen concentration, the concentration of active catalyst is reduced.

The rates of alcohol oxidation by all of the Os−Cr and Ru−Cr complexes were similar but did depend on both the metal, Os or Ru, and the ligands around that metal. Bulky alkyl groups on the osmium or ruthenium center reduced the rate of the alcohol oxidation reaction. Steric bulk at this metal would impede coordination of alcohol. For complexes with the same alkyl ligands, the Ru−Cr complexes are better catalysts than the Os−Cr analogues. We attribute this to the increased lability of the second row metal over the third row metal.

The oxidation of dppe by **1** clearly proceeds through a different pathway than does the oxidation of alcohols by the catalyst (Scheme 9). In this reaction, the terminal oxo groups on the chromium center transfer to the coordinated diphosphine. Molecular oxygen reoxidizes the reduced chromium unit and, with labeled molecular oxygen, scrambles with the bridge and terminal oxo ligands. The chromium oxo complex $CrO(H_2O)_x^{2+}$, formed from the reaction of O_2 with Cr(II) in aqueous solution, oxidizes PPh_3 to $O{=}PPh_3$.[10] Free phosphines react with other oxo−metal complexes to generate phosphine oxide by an attack of the phosphine on a terminal oxo group, followed by displacement of phosphine oxide from the complex.[42] Unlike **1**, there is no Os−Cr interaction in **7**, and the chromate group in this molecule would be more likely to react as a free chromate ion and oxidize phosphines.

(40) Halpern, *J. Inorg. Chim. Acta* **1982**, *62*, 31−37.
(41) Karlin, K. D.; Gultneh, Y. *Prog. Inorg. Chem.* **1987**, *35*, 219.

Scheme 9. Proposed Catalytical Cycle for the Oxidation of dppe by **1**

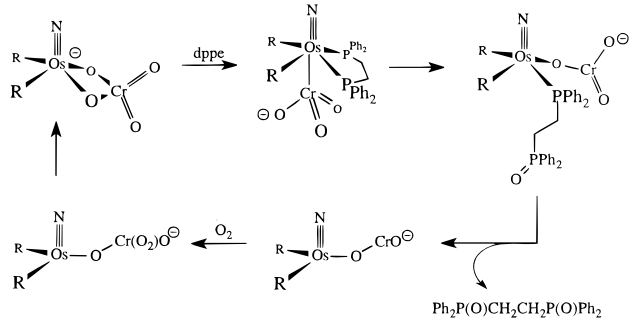

Conclusion

We prepared a series of heterobimetallic complexes containing a chromate anion chelated to a nitrido(dialkyl)ruthenium(VI) or a nitrido(dialkyl)osmium(VI) center. These complexes are selective alcohol oxidation catalysts. They oxidize primary and secondary alcohols to the corresponding carbonyl compounds using molecular oxygen. The evidence points to a mechanism for oxidation that involves initial coordination of the alcohol to the osmium or ruthenium center, proton transfer from alcohol to a bridging oxo group, and β-hydrogen elimination.

Experimental Section

All reactions were conducted under N_2 using standard air-sensitive techniques unless otherwise indicated. Anhydrous $(C_2H_5)_2O$, THF, and C_6H_{14} were distilled from Na/benzophenone, while $C_6H_5CH_3$ was distilled from Na. CH_2Cl_2 and CH_3CN were distilled from CaH_2. The corresponding deuterated solvents were dried in the same manner and were stored over 4-Å molecular sieves. The compounds $[N(n\text{-}Bu)_4][Os(N)(CH_2SiMe_3)_2Cl_2]$,[17] $[PPh_4][Os(N)(CH_2SiMe_3)_2Cl_2]$, $[N(n\text{-}Bu)_4][Ru(N)(CH_2SiMe_3)_2Cl_2]$, $[PPh_4][Os(N)(CH_3)_2Cl_2]$, $[PPh_4][Ru(N)(CH_3)_2Cl_2]$,[19] $[N(n\text{-}Bu)_4][Os(N)(CH_2SiMe_3)_2(SO_4)]$, $[N(n\text{-}Bu)_4][Os(N)(CH_2SiMe_3)_2(CO_3)]$,[28] $[Os(N)(CH_2SiMe_3)_2(dppe)(NCMe)][BF_4]$,[43] $[N(n\text{-}Bu)_4][Os(N)(CH_2SiMe_3)_2(dppe)CrO_4]$, and $[PPh_4][Os(N)(CH_2SiMe_3)_2(dppe)CrO_4]$[16] were prepared according to literature methods.

NMR spectra were recorded on one of the following spectrometers: GE QE300, Varian U-400, or GE GN500 FT NMR. IR spectra were recorded on a Perkin-Elmer 1600 series FTIR spectrophotometer. Electronic spectra were recorded on a Hewlett-Packard 8452A diode array UV−visible spectrophotometer. Gas chromatographic experiments were performed on a Hewlett-Packard 5790 series gas chromatograph. Elemental analyses were performed at the University of Illinois School of Chemical Sciences Microanalytical Laboratory. Mass spectra were recorded at the University of Illinois School of Chemical Sciences Mass Spectrometry Laboratory. Electrochemical measurements were made with a BAS 100 electrochemical analyzer. All electrochemistry was done in a Vacuum Atmospheres drybox. Measurements were taken on an approximately 0.01 M solution of the compound of interest using $[N(n\text{-}Bu)_4][BF_4]$ as the supporting electrolyte. A solution of 0.1 M $[N(n\text{-}Bu)_4][BF_4]$ in CH_2Cl_2 was prepared from freshly distilled solvent. Potentials are reported vs Ag/AgCl.

Synthesis of $[N(n\text{-}Bu)_4][Os(N)(CH_2SiMe_3)_2(\mu\text{-}O)_2CrO_2]$ (1a). Method A. An orange solution of $[N(n\text{-}Bu)_4][Os(N)(CH_2SiMe_3)_2Cl_2]$ (0.040 g, 0.058 mmol) in 30 mL of CH_2Cl_2 was added to solid Ag_2CrO_4 (0.076 g, 0.23 mmol) in a 100-mL flask, and the flask was closed with a septum cap. The heterogeneous mixture was magnetically stirred

(42) (a) Cheng, S. Y. S.; James, B. R. *J. Mol. Catal. A* **1997**, *117*, 91−102. (b) Lemaux, P.; Bahri, H.; Simonneaux, G.; Toupet, L. *Inorg. Chem.* **1995**, *34*, 4691−4697. (c) Che, C.-M.; Wong, K.-Y. *J. Chem. Soc., Dalton Trans.* **1989**, 2065−2067. (d) Groves, J. T.; Ahn, K.-H. *Inorg. Chem.* **1987**, *26*, 3831−3833. (e) Moyer, B. A.; Sipe, B. K.; Meyer, T. J. *Inorg. Chem.* **1981**, *20*, 1475−1480.
(43) Shapley, P. A.; Schwab, J. J.; Wilson, S. R. *J. Coord. Chem.* **1994**, *32*, 213−232.

under a low-intensity UV lamp (model UVGL-25 Mineralight lamp) for 12 h. The color of the solution changed from orange to brown within 1 h. After 12 h, the solution was dark purple. The mixture was filtered. Solvent was removed from the purple filtrate under vacuum. The residue was dissolved in a few milliliters of CH_2Cl_2. The volume was doubled with hexane, and the solution was filtered. The solution was cooled to −30 °C, and red-purple crystals formed. The crystals were collected in a fritted glass filter and dried under vacuum to give analytically pure $[N(n\text{-}Bu)_4][Os(N)(CH_2SiMe_3)_2(\mu\text{-}O)_2CrO_2]$ (0.040 g, 0.054 mmol, 94% yield).

When a mixture of $[N(n\text{-}Bu)_4][Os(N)(CH_2SiMe_3)_2Cl_2]$ ((0.040 g, 0.058 mmol) and Ag_2CrO_4 (0.076 g, 0.23 mmol)) in 30 mL of CH_2Cl_2 was stirred for 24 h in an aluminum foil covered flask, there was no reaction, and starting material was recovered. Under ambient light, conversion of reactants to $[N(n\text{-}Bu)_4][Os(N)(CH_2SiMe_3)_2(\mu\text{-}O)_2CrO_2]$ required 3−7 d.

Method B. To a 100-mL round flask were added a solution of $[N(n\text{-}Bu)_4][Os(N)(CH_2SiMe_3)_2Cl_2]$ (0.50 g, 0.72 mmol) and $[N(n\text{-}Bu)_4]Br$ (0.4 g, 1.24 mmol) in 60 mL of CH_2Cl_2 and a solution of K_2CrO_4 (1 g, 5.2 mmol) in 15 mL of H_2O. The mixture was loosely capped (in air) and stirred for 3 d at room temperature. The mixture was transferred to a separatory funnel. It consisted of a violet-purple organic layer and a bright yellow aqueous layer. The organic layer was separated, washed with water (3 × 20 mL), and dried over anhydrous $MgSO_4$. The solvent was removed under vacuum. The residue was purified either by crystallization as above or by column chromatography on silica gel (10% CH_3CN in CH_2Cl_2 eluant). Purple crystals (0.040 g, 0.54 mmol, 75%) were obtained. IR (KBr, cm^{-1}): 1111 (s, Os−N), 948 (vs, Cr−O), 928 (vs, Cr−O). ^1H NMR (CD_2Cl_2, 500 MHz, 293 K): δ 3.18 (m, 4H, $NCH_2CH_2CH_2CH_3$), 2.08 (s, 2H, $OsCH_2$), 1.63 (m, 4H, NCH_2CH_2), 1.43 (m, 4H, $NCH_2CH_2CH_2CH_3$), 1.02 (t, 6H, $NCH_2CH_2CH_2CH_3$), 0.09 (s, 9H, $SiCH_3$). $^{13}C\{1H\}$ NMR (CD_2Cl_2, 125.76 MHz, 293 K): δ 59.27 ($NCH_2CH_2CH_2CH_3$), 24.25 ($NCH_2CH_2CH_2CH_3$), 20.12 ($NCH_2CH_2CH_2$-CH_3), 13.78 ($NCH_2CH_2CH_2CH_3$), 5.59 ($OsCH_2$), 0.81 ($SiCH_3$). Anal. Calcd for $OsCrN_2Si_2O_4C_{24}H_{58}$: C, 39.11; H, 7.93; N, 3.80. Found: C, 39.07; H, 8.02; N, 3.81. Melting point: 119 °C. Decomposition: 180 °C. UV−visible (λ_{max}, nm, CH_2Cl_2 (ϵ)): 350 (3741), 504 (2667).

Synthesis of $[PPh_4][Os(N)(CH_2SiMe_3)_2(\mu\text{-}O)_2CrO_2]$ (1b). In a 50-mL round-bottom flask, a solution of $[PPh_4][Os(N)(CH_2SiMe_3)_2Cl_2]$ (0.100 g, 0.127 mmol) in 35 mL of CH_2Cl_2 was stirred vigorously with a 5-mL solution of K_2CrO_4 (0.235 g, 1.21 mmol) in H_2O. The mixture was stirred vigorously for 3 d, and aliquots were taken periodically and examined by ^1H NMR spectroscopy. The reaction mixture was transferred to a separatory funnel, and the two phases were separated. The organic phase was washed once with 15 mL of H_2O and dried over anhydrous Na_2SO_4. Solvent was removed from the purple filtrate under vacuum. The residue was dissolved in a few milliliters of CH_2Cl_2. Hexane was added dropwise until the solution became cloudy, and the solution was filtered. The solution was cooled to −30 °C, and purple crystals formed. Purple crystals (0.065 g, 0.078 mmol, 61%) were obtained. IR (KBr, cm^{-1}): 1122 (s, $\nu_{Os\equiv N}$), 1108 (s, δ_{PC}), 956 (vs, $\nu_{Cr=O}$), 926 (vs, $\nu_{Cr=O}$). ^1H NMR (300 MHz, $CDCl_3$, 20 °C): δ 7.64−7.78 (m, 20H, Ph), 2.07 (d, J = 10.6 Hz, 2H, $OsCH^aH^b$), 1.99 (d, J = 10.6 Hz, 2H, $OsCH^aH^b$), 0.062 (s, 18H, $SiCH_3$). MS (ES, m/z): 495.9 [$(CH_3SiCH_2)_2(N)Os(\mu\text{-}O_2)CrO_2]^-$. Melting point: 136 °C.

Synthesis of $[N(n\text{-}Bu)_4][RuN(CH_2SiMe_3)_2(\mu\text{-}O_2)CrO_2]$ (2). A solution of $[N(n\text{-}Bu)_4][Ru(N)(CH_2SiMe_3)_2Cl_2]$ (0.020 g, 0.033 mmol) in 5 mL of CH_2Cl_2 was added dropwise to a suspension of Ag_2CrO_4 (0.022 g, 0.066 mmol) in 30 mL of CH_2Cl_2. The mixture was stirred under a low-intensity UV lamp (model UVGL-25 Mineralight lamp) for 60 h, and then solvent was removed under vacuum, and the residue was extracted with CH_2Cl_2 and filtered. Hexane was added to the filtrate, and it was cooled to −30 °C. Brown crystals (0.011 g, 0.017 mmol, 51%) were collected and dried under vacuum. IR (KBr, cm^{-1}): 1082 (s, ν_{Ru-N}), 944 (vs, $\nu_{Cr=O}$), 923 (vs, $\nu_{Cr=O}$). ^1H NMR ($CDCl_3$, 200 M Hz, 294 K): δ 3.31 (m, 8H, NCH_2), 1.72 (d, 2H, J = 10 Hz, $OsCH^aH^b$), 1.68 (d, 2H, J = 10 Hz, $OsCH^aH^b$), 1.65−1.41 (m, 16H, $NCH_2CH_2CH_2$-CH_3), 0.98 (t, 12H, $NCH_2CH_2CH_2CH_3$), 0.05 (s, 18H, $SiCH_3$). $^{13}C\{^1H\}$NMR ($CDCl_3$, 75.5 MHz, 295 K): δ 58.41 (NCH_2), 23.57 ($NCH_2CH_2CH_2CH_3$), 19.40 ($NCH_2CH_2CH_2CH_3$), 13.33 (NCH_2CH_2-CH_2CH_3), 11.64 ($OsCH_2$), 0.384 ($SiCH_3$). Anal. Calcd for $RuCrN_2O_4Si_2C_{24}H_{58}$: C, 44.49; H, 9.02; N, 4.32. Found: C, 44.29; H, 8.98; N, 4.14. UV−visible (λ_{max}, nm, CH_2Cl_2 (ϵ)): 356 nm (1708). Melting point: 95−96 °C. Decomposition: 124 °C.

Synthesis of $[PPh_4][Os(N)Me_2(\mu\text{-}O_2)CrO_2]$ (3). To a solution of $[PPh_4][NOsMe_2Cl_2]$ (0.080 g, 0.12 mmol) in 20 mL of CH_2Cl_2 was added excess Ag_2CrO_4 (0.080 g, 0.24 mmol). The solution was stirred under a low-intensity UV lamp (model UVGL-25 Mineralight lamp) for 4.5 h. The dark purple solution was filtered and concentrated to 3 mL under vacuum. Diethyl ether was added, and the solution was cooled to −30 °C. Cotton-like purple crystals (0.076 g, 0.11 mmol, 92%) were collected and dried under vacuum. IR (KBr, pellet, cm^{-1}): 1109 (s, Os−N), 956 (vs, Cr−O), 922 (vs, Cr−O), 795 (m, Cr−O). ^1H NMR ($CDCl_3$, 200 MHz, 293 K): δ 2.25 (s, 3H, $OsCH_3$), 7.95−7.55 (m, 10H, PPh). Anal. Calcd for $OsCrNPO_4C_{26}H_{26}$: C, 45.28; H, 3.80; N, 2.03. Found: C, 45.11; H, 3.85; N, 1.94.

Preparation of $[PPh_4][Ru(N)Me_2(\mu\text{-}O_2)CrO_2]$ (4). Method A. Orange crystals of $[PPh_4][Ru(N)(CH_3)_2Cl_2]$ (0.180 g, 0.32 mmol) were dissolved in 50 mL of CH_2Cl_2. Two equivalents of Ag_2CrO_4 (0.22 g, 0.65 mmol) was added, and the mixture was stirred for 4 d at room temperature. The heterogeneous mixture was filtered to yield a red-brown solution. The solvent was removed under vacuum, and the residue was dissolved in 15 mL of CH_2Cl_2. Pentane was added, and the solution was cooled to −30 °C. Crystals of **4** (0.17 g, 0.29 mmol, 89%) were collected by filtration and dried under vacuum.

Method B. A solution of $[PPh_4][Ru(N)Me_2Br_2]$ (0.010 g, 0.016 mmol) in 5 mL of CH_2Cl_2 was added to an aqueous solution of K_2CrO_4 (0.030 g, 0.15 mmol, 5 mL H_2O). The mixture was stirred at room temperature for 2 h under air. The organic layer was separated and filtered. Solvent was removed under vacuum. The residue consisted of a deep orange solid. The product, $[PPh_4][RuNMe_2CrO_4]$ (0.007 g, 0.012 mmol, 73%), was obtained after crystallization from CH_2Cl_2/C_6H_{14}. IR (KBr, pellet, cm^{-1}): 1087 (s, Ru−N), 953 (vs, Cr−O), 923 (vs, Cr−O), 810 (m, Cr−O). ^1H NMR (CD_2Cl_2, 300 MHz, 293 K): δ 8.0−7.5 (m, 10H, PPh), 1.76 (s, 3H, $RuCH_3$). ^1H NMR (400 MHz, $CDCl_3$, 16.9 °C): δ 7.92 (m, 4H, $p\text{-}PC_6H_5$), 7.77 (m, 8H, $o\text{-}PC_6H_5$), 7.60 (m, 8H, $m\text{-}PC_6H_5$), 1.78 (s, 6H, $RuCH_3$). $^{13}C\{^1H\}$ NMR (100 MHz, $CDCl_3$, 16.9 °C): δ 135.72 (d, $p\text{-}C_6H_5$, J = 2.3 Hz), 134.39 (d, $m\text{-}PC_6H_5$, J = 9.9 Hz), 130.69 (d, $o\text{-}PC_6H_5$, J = 12.9 Hz), 117.42 (d, ipso-PC_6H_5, J = 89.5 Hz), 3.55 (s, $RuCH_3$). UV−visible (λ_{max}, nm, CH_2Cl_2 (ϵ)): 354 (2422). Anal. Calcd for $C_{26}H_{26}NRuO_4PCr$: C, 52.00; H, 4.36; N, 2.33. Found: C, 52.05; H, 4.36; N, 2.34.

Preparation of $[N(n\text{-}Bu)_4][Os(N)(C_6H_5)_4]$. Purple crystals of $[N(n\text{-}Bu)_4][Os(N)Cl_4]$ (0.150 g, 0.26 mmol) were suspended in 40 mL of a 1:1 mixture of diethyl ether/THF. A THF solution of PhMgCl (2.0 M, 0.56 mL, 1.12 mmol) was added to the mixture with stirring. The solution immediately turned orange and then yellow. After 5 min, the mixture was filtered, and solvent was removed under vacuum. The residue was dissolved in CH_2Cl_2 and filtered through Celite. Hexane was added, and the solution was cooled to −30 °C. Yellow needles (0.171 g, 0.23 mmol, 89%) were collected and dried under vacuum. IR (KBr, cm^{-1}): 3049 (w, phenyl ν_{CH}), 2963 (m, ν_{CH}), 2932 (w, ν_{CH}), 2874 (w, ν_{CH}), 1568 (s), 1560 (w), 1481 (m), 1472 (m, δ_{CH}), 1458 (m), 1420 (w), 1382 (w, δ_{CH}), 1252 (w), 1177 (w), 1151 (w), 1123 (m, $\nu_{Os\equiv N}$), 1062 (m), 1020 (s), 882 (w), 734 (s, δ_{ar-CH}), 700 (s, δ_{ar-CH}), 647 (w, δ_{ar-CH}). ^1H NMR (500 MHz, $CDCl_3$, 19.8 °C): δ 7.23 (m, 2H, $m\text{-}C_6H_5$), 6.68 (m, 2H, $o\text{-}C_6H_5$), 6.92 (m, 1H, $p\text{-}C_6H_5$), 2.58 (m, 2H, $NCH_2CH_2CH_2CH_3$), 1.27 (m, 4H, $NCH_2CH_2CH_2CH_3$), 0.97 (t, 3H, J = 6.82 Hz, $NCH_2CH_2CH_2CH_3$). $^{13}C\{^1H\}$ NMR (125.76 MHz, $CDCl_3$, 19.8 °C): δ 168.9 ($i\text{-}C_6H_5$), 139.6 (Ph), 126.6 (Ph), 121.6 ($p\text{-}C_6H_5$), 58.3 ($NCH_2CH_2CH_2CH_3$), 23.9 ($NCH_2CH_2CH_2CH_3$), 19.6 (NCH_2-$CH_2CH_2CH_3$), 13.7 ($NCH_2CH_2CH_2CH_3$). Anal. Calcd for $C_{40}H_{56}N_2Os$: H, 7.48; C, 63.63; N, 3.71. Found: H, 7.66; C, 63.54; N, 4.01. Decomposition: 170 °C.

Preparation of $[N(n\text{-}Bu)_4][Os(N)(C_6H_5)_2Cl_2]$. A solution of HCl in $(C_2H_5)_2O$ (1.0 M, 0.38 mL, 0.38 mmol) was added dropwise to a stirred solution of $[N(n\text{-}Bu)_4][(C_6H_5)_4Os(N)]$ (0.142 g, 0.188 mmol) in 30 mL of CH_2Cl_2. After 15 min, the solution was concentrated under vacuum to 5 mL. Hexane was added, and the solution was cooled to −30 °C. Orange crystals (0.099 g, 0.15 mmol, 78%) were collected and dried under vacuum. IR (KBr, cm^{-1}): 3053 (w, phenyl ν_{CH}), 2962 (s, ν_{CH}), 2932 (m, ν_{CH}), 2873 (m, ν_{CH}), 1482 (s), 1468 (m), 1381 (w),

1152 (w), 1130 (m, ν_{OsN}), 1070 (m), 1063 (m), 1022 (m), 884 (w), 744 (s, δ_{ar-CH}), 735 (s, δ_{ar-CH}), 701 (m, δ_{ar-CH}), 696 (m, δ_{ar-CH}). ^{1}H NMR (500 MHz, $CDCl_3$): δ 7.1 (m, 2H, *m*-C_6H_5), 6.9 (m, 2H, *o*-C_6H_5), 6.7 (m, 1H, *p*-C_6H_5), 3.1 (m, 2H, $NCH_2CH_2CH_2CH_3$), 1.6 (m, 2H, $NCH_2CH_2CH_2CH_3$), 1.4 (m, 2H, $NCH_2CH_2CH_2CH_3$), 1.0 (t, 3H, $NCH_2CH_2CH_2CH_3$). ^{13}C{^{1}H} NMR (125.76 MHz, $CDCl_3$): δ 151.9 (*i*-C_6H_5), 136.8 (*m*-C_6H_5), 127.4 (*o*-C_6H_5), 123.9 (*p*-C_6H_5), 58.7 ($NCH_2CH_2CH_2CH_3$), 24.0 ($NCH_2CH_2CH_2CH_3$), 19.7 ($NCH_2CH_2CH_2CH_3$), 13.7 ($NCH_2CH_2CH_2CH_3$). UV−visible (λ_{max}, nm, CH_2Cl_2 (ϵ)): 452 (305). Anal. Calcd for $C_{28}H_{46}N_2Cl_2Os$: H, 6.9; C, 50.06; N, 4.17. Found H, 7.17; C, 49.68; N, 4.30. Melting point: 136 °C.

Preparation of [N(*n*-Bu)$_4$][Os(N)Ph$_2$(μ-O$_2$)CrO$_2$] (5). A solution of [N(*n*-Bu)$_4$][(C_6H_5)$_2$(N)OsCl$_2$] (0.107 g, 0.159 mmol) in 15 mL of CH_2Cl_2 was combined with a solution of K_2CrO_4 (0.195 g, 1.0 mmol) in 15 mL of H_2O in a 100-mL flask. The solution was stirred at room temperature under air for 4 d. The organic layer was separated and dried over anhydrous $MgSO_4$. The solvent was evaporated under vacuum to give a purple, oily residue (0.098 g, 0.136 mmol, 86%). The product was pure by ^{1}H NMR spectroscopy. IR (KBr, cm^{-1}): 1120 (s, ν_{OsN}), 901 (ν_{CrO}), 893 (ν_{CrO}). ^{1}H NMR (300 MHz, CD_2Cl_2, 24 °C): δ 7.27 (d, J = 7.7 Hz, 4H, Ph), 7.14 (t, J = 7.4 Hz, 4H, Ph), 7.03 (m, 2H, Ph), 3.06 (m, 8H, $NCH_2CH_2CH_2CH_3$), 1.53 (m, 8H, $NCH_2CH_2CH_2CH_3$), 1.37 (m, 8H, $NCH_2CH_2CH_2CH_3$), 0.99 (t, 12H, J = 7.1 Hz, $NCH_2CH_2CH_2CH_3$). ^{13}C{^{1}H} NMR (125.76 MHz, CD_2Cl_2, 20 °C): δ 139.3, 128.4, 125.6, 59.1 ($NCH_2CH_2CH_2CH_3$), 24.1 ($NCH_2CH_2CH_2CH_3$), 20.1 ($NCH_2CH_2CH_2CH_3$), 13.8 ($NCH_2CH_2CH_2CH_3$). UV−visible (λ_{max}, nm, CH_2Cl_2 (ϵ)): 520 (1500).

Preparation of [PPh$_4$][Os(N)Me$_3$(CH$_2$SiMe$_3$)]. A solution of Mg(CH_2SiMe_3)$_2$ (0.30 mmol) in 5 mL of diethyl ether was added to a stirred suspension of [PPh_4][$OsNMe_3Cl$] (0.188 g, 0.301 mmol) in 20 mL of diethyl ether with stirring. After 0.5 h, the reaction mixture was filtered through Celite. The yellow filtrate was concentrated to approximately 12 mL under vacuum, hexane was added, and the mixture was cooled to −30 °C. Yellow-orange crystals of [PPh_4][Os(N)Me_3(CH_2SiMe_3)] were collected and dried under vacuum (0.054 g, 32%). ^{1}H NMR (400 MHz, $CDCl_3$, 21 °C): δ 7.95−7.55 (m, 20H, P(C_6H_5), 1.30 (s, 6H, CH_3), 1.27 (s, 3H, CH_3), 0.97 (s, 2H, CH_2SiMe_3), 0.03 (s, 9H, $CH_2Si(CH_3)_3$). ^{13}C{^{1}H} NMR (125.6 MHz, $CDCl_3$, 22.4 °C): δ 135.9 (d, J = 6.4 Hz, *p*-Ph), 134.4 (d, J = 10.2 Hz, *m*-Ph), 130.8 (d, J = 12.9 Hz, *o*-Ph), 117.4 (d, J = 89.2 Hz, *q*-Ph), 13.3 (CH_2SiMe_3), 4.6 (*cis*-CH_3), 3.9 (*trans*-CH_3), 1.9 ($CH_2Si(CH_3)_3$). Anal. Calcd for $C_{31}H_{40}NOsPSi$: C, 55.09; H, 5.96; N, 2.07. Found: C, 55.05; H, 5.93; N, 1.90.

Preparation of [PPh$_4$][Os(N)Me(CH$_2$SiMe$_3$)Cl$_2$]. Solid [C_5H_5NH][Cl] (0.018 g, 0.160 mmol) was added to a stirred solution of [PPh_4][Os(N)Me_3(CH_2SiMe_3)] (0.045 g, 0.067 mmol) in 10 mL of CH_2Cl_2. The color or the solution changed from yellow to orange within minutes. After 0.5 h, the solvent and pyridine were removed under vacuum. The residue was extracted with 10 mL of THF, and the extract was filtered through Celite. The THF solution was concentrated to approximately 2 mL, and diethyl ether was added to precipitate [PPh_4][Os(N)Me_2Cl_2]. The mixture was filtered. The solvent was removed from the filtrate under vacuum, and the residue was crystallized from THF/hexane at −30 °C. Red crystals of [PPh_4][Os(N)Me(CH_2SiMe_3)Cl_2] (xx g, xx mmol) were collected and dried under vacuum. ^{1}H NMR (400 MHz, $CDCl_3$, 27.0 °C): δ 7.95−7.60 (m, 20H, P(C_6H_5)$_4$), 2.80 (q, J_{AB} = 8.4 Hz, 2H, Os$CH^AH^BSiMe_3$), 2.66 (s, 3H, OsCH_3), 0.03 (s, 9H, $OsCH_2Si(CH_3)_3$). ^{13}C{^{1}H} NMR (125.6 MHz, $CDCl_3$, 22.4 °C): δ 135.8 (s, *p*-Ph), 134.7 (d, J = 10.1 Hz, *m*-Ph), 130.9 (d, J = 12.9 Hz, *o*-Ph), 117.5 (d, J = 90.2 Hz, *q*-Ph), 10.3 (s, CH_2SiMe_3), 2.2 (s, *C*H3), 0.3 (s, $CH_2Si(CH_3)_3$).

Synthesis of [PPh$_4$][Os(N)Me(CH$_2$SiMe$_3$)(μ-O$_2$)CrO$_2$] (6). In a 5-mL vial, a solution of [PPh_4][Os(N)Me(CH_2SiMe_3)Cl_2] (0.010 g, 0.014 mmol) in 2 mL of CH_2Cl_2 was stirred vigorously with Ag_2CrO_4 (0.010 g, 0.030 mmol) in sunlight for 7 d. The solution changed from orange to deep purple. The mixture was filtered. Diethyl ether was added to the filtrate, and it was cooled to −30 °C. Purple crystals (0.009 g, 0.012 mmol, 86%) were collected. ^{1}H NMR (500 MHz, $CDCl_3$, 21.7 °C): δ 7.95−7.60 (m, 20H, P(C_6H_5)$_4$), 2.28 (s, 3H, OsCH_3), 2.18 (d, J = 10.5 Hz, 1H, $OsCH_2SiMe_3$), 1.62 (d, J = 10 Hz, 1H, $OsCH_2SiMe_3$), 0.31 (s, 9H, $OsCH_2Si(CH_3)_3$). ^{13}C{^{1}H} NMR (125.6 MHz, $CDCl_3$, 21.7 °C): δ 135.7 (d, J = 4 Hz, *p*-Ph), 134.5 (d, J = 10.2 Hz, *m*-Ph), 130.7 (d, J = 12.9 Hz, *o*-Ph), 117.5 (d, J = 90.2 Hz, *q*-Ph), 4.9 (s, CH_3), 0.48 (s, $CH_2Si(CH_3)_3$), −2.2 (s, CH_3SiM). IR (CH_2Cl_2 solution, cm^{-1}): 1115 (s, Os≡N), 957 (vs, Cr═O), 928 (vs, Cr═O). UV−vis (λ_{max}, nm, CH_2Cl_2) 348, 498 (v br). Mass spectrum (ESI, CH_3CN solution, *m*/*z*): 424.2 ([$CrOsNSiO_4C_5H_{14}$]$^-$).

Structure Determination of 2. A transparent, orange, platy crystal, grown from CH_2Cl_2/C_6H_{14} solution, of dimensions 0.03 mm × 0.1 mm × 0.6 mm was used. The crystal was bound by the forms {0 1 0} and {0 0 1} and faces {−1 0 −3}, {−1 0 2}, and {1 0 0}. Distances from the crystal center to these facial boundaries were 0.015, 0.07, 0.18, 0.25, and 0.31 mm, respectively. The sample uniformly extinguished plane-polarized light. An Enraf-Nonius CAD4 automated *k*-axis diffractometer with graphite crystal monochromator was used. The crystal was triclinic, space group $P\bar{1}$, and there were two molecules per unit cell. The structure was solved by Patterson methods (SHELXS-86); correct ruthenium and chromium atom positions were deduced from a vector map, and partial structure expansion gave positions for the oxygen, N1, C1, and C2 atomic positions.[44] Subsequent least-squares difference Fourier calculations revealed positions for the remaining nonhydrogen atom positions. Hydrogen atom were included as fixed contributors in idealized positions. In the final cycle of least squares, anisotropic thermal coefficients were refined for the non-hydrogen atoms, and group isotropic thermal parameters were varied for the methyl and methylene hydrogen atoms. The high thermal parameter associated with the methyl hydrogen atoms may indicate a possible disorder. Successful convergence was indicated by the maximum shift/error for the last cycle. There were no significant features in the final difference Fourier map. A final analysis of variance between observed and calculated structure factors showed no apparent systematic errors. The final agreement factors were R = 0.048 and R_w = 0.061.

Structure Determination of 6. Crystals were grown from CH_2Cl_2/C_6H_{14}. The data crystal was mounted using oil (Paratone-N, Exxon) to a thin glass fiber with the (0 −1 0) scattering planes roughly normal to the spindle axis. Systematic conditions suggested the unambiguous space group. Structure was solved by Patterson methods.[45] The proposed model includes both enantiomers in equal proportions. The space group choice was confirmed by successful convergence of the full-matrix least-squares refinement on F^2.[46] The highest peaks in the final difference Fourier map were in the vicinity of Os; the final map had no other significant features. A final analysis of variance between observed and calculated structure factors showed no dependence on amplitude or resolution. Crystal data for **2a** and **6b** are summarized in Table 4.

Reaction of 1a with HBF$_4$·O(CH$_3$)$_2$. In a 5-mm NMR tube, **1a** (0.007 g, 0.0095 mmoL) was dissolved in 0.6 mL of toluene-d_8. One equivalent of HBF_4·$O(CH_3)_2$ (0.972 μL, 0.0095 mmoL) was injected by syringe. The color of the solution immediately changed from purple to dark blue. A ^{1}H NMR spectrum showed only very broad peaks for the N(*n*-Bu)$_4$ cation and Me_2O. IR (KBr, cm^{-1}): 3433 (m, O−H), 1111 (s, Os≡N), 950 (vs, Cr═O), 927 (vs, Cr═O). ESR-300 (toluene): g_1 = 4.1856, g_2 = 1.9983. UV−visible (λ_{max}, nm, toluene): 540, 660 (v br).

Reaction of 1a with HCl$_{(aq)}$. A solution of **1a** (0.020 g, 0.027 mmol) in 10 mL of CH_2Cl_2 was cooled to 0 °C under air. An aqueous solution of HCl (0.5 mL, 12 M) was added, and the mixture was stirred. The color of the organic layer immediately changed from purple to blue. The mixture was warmed to room temperature and stirred for 1 d. The organic layer slowly changed to orange. The aqueous solution was yellow-brown. The orange organic layer was separated, and solvent was removed under vacuum. The residue was crystallized from (C_2H_5)$_2$O/C_6H_{14} to give [N(*n*-Bu)$_4$][Os(N)(CH_2SiMe_3)$_2Cl_2$] (0.012 g, 0.017 mmol, 64%). ^{1}H NMR spectroscopy showed this to be the cis isomer.

(44) (a) Sheldrick, G. M., Kruger, C., Goddard, R., Eds. SHELX-86. In *Crystallographic Computing 3*; Oxford University: Oxford, UK, 1985; pp 175−189. (b) Ibers, J. A., Hamilton, W. C., Eds. *International Tables for X-ray Crystallography*; Kynoch: Birmingham, England, 1974; Vol. IV, pp 61−66, 99−101, 149−150.

(45) Sheldrick, G. M. SHELXS-86. *Acta Crystallogr.* **1990**, *A46*, 467−473.

(46) Sheldrick, G. M. *SHELXL-93*; Program for crystal structure refinement. Institute fur Anorg. Chemie: Gottingen, Germany, 1993.

Table 4. Summary of Crystal Data for **2a** and **6b**

	2a	6bxe1 CH_2Cl_2
chemical formula	$RuCrSi_2O_4N_2C_{24}H_{58}$	$OsCrPSiCl_2O_4C_{30}H_{36}$
space group	$P\bar{1}$	$P2_12_12_1$
a, Å	10.013(2)	9.41350(10)
b, Å	10.192(2)	10.81600(10)
c, Å	17.726(4)	33.35820(10)
α, deg	104.87(1)	90
β, deg	94.40(1)	90
γ, deg	98.80(1)	90
V, Å^3	1715(1)	3396.41(5)
Z	2	4
density calcd, g/cm^3	1.255	1.656
temperature, K	300	198
radiation	Mo Kα (graphite) $K\alpha_1 = 0.709\ 30$, $K\alpha_2 = 0.713\ 59$ $\lambda = 0.710\ 73$ Å	
abs coeff (m), cm^{-1}	60.75	43.31
collection method	1.50 (1.00 + 0.35 tan ϕ) deg ω, variable from 3 to 16 deg/min‘	0.25 deg/ω scans, 0.3333 min/scan
reflections with $I > 2.58\sigma(I)$	5001	6830
R	0.048	0.0470
R_w	0.061	0.0721

Reaction of 1a with $CH_3OSO_2CF_3$. A solution of $CH_3OSO_2CF_3$ (7.8 μL, 0.068 mmol) in 10 mL of $(C_2H_5)_2O$ was added dropwise to a solution of **1a** (0.050 g, 0.068 mmol) in 10 mL of THF at −78 °C. The mixture was stirred at −78 °C for 10 h. The color of solution changed from purple to deep blue. The solution was warmed to room temperature. Solvent was removed under vacuum to give a blue oil. A ^{1}H NMR spectrum in C_6D_6 showed only very broad peaks for the N(*n*-Bu)$_4$ cation. IR (KBr, cm^{-1}): 1108 (s, Os≡N), 951 (s, Cr═O), 917 (s, Cr═O). UV−visible (λ_{max}, nm, toluene): 540, 660 (v br).

Preparation of [N(*n*-Bu)$_4$][Os(N)(CH$_2$SiMe$_3$)$_2$(SO$_4$)(dppe)]. A solution containing [N(*n*-Bu)$_4$][Os(N)(CH$_2$SiMe$_3$)$_2$(SO$_4$)] (0.053 g, 0.074 mmol) and dppe (0.030 g, 0.075 mmol) in 10 mL of CH_2Cl_2 was stirred for 20 min. The solvent was removed under vacuum, and the yellow residue was dissolved in 1 mL of $(C_2H_5)_2O$. The solution was cooled to −30 °C. Hexane was added, and yellow crystals (0.064 g, 0.057 mmol, 76%) formed. IR (KBr, cm^{-1}): 3055 (w, phenyl ν_{CH}), 2961 (m, ν_{CH}), 2876 (m, ν_{CH}), 1436 (m, δ_{CH}), 1255 (w), 1241 (m, δ_{Si-C} sym), 1144 (s, ν_{SO}), 1119 (s, ν_{OsN}), 1090 (s, ν_{SO}), 1028 (w), 1000 (w), 856 (s, γ_{SiCH_3}), 829 (s, γ_{SiCH_3}), 745 (m δ_{ar-CH}), 692 (m δ_{ar-CH}), 678 (w), 618 (s), 528 (m), 518 (m), 487 (w). ^{1}H NMR (300 MHz, C_6D_6, 20.8 °C): δ 7.0−8.0 (m, 10H, Ph), 3.65 (m, 1H, PC*H*^{a}H^b), 3.38 (m, 4 H, NC*H*$_2$CH$_2$CH$_2$CH$_3$), 2.68 (m, 1H, PCH^a*H*^{b}), 2.26 (m, 1H, OsC*H*^{a}H^b), 2.20 (m, 1H, OsCH^a*H*^{b}), 1.63 (m, 4H, NCH$_2$C*H*$_2$CH$_2$CH$_3$), 1.45 (m, 4H, NCH$_2$CH$_2$C*H*$_2$CH$_3$), 0.986 (t, 6H, $J = 7.2$ Hz, NCH$_2$CH$_2$CH$_2$C*H*$_3$), −0.22 (s, 9H, SiCH$_3$). ^{13}C{^{1}H} NMR (125.76 MHz, $CDCl_3$, 19.8 °C): δ 134.53 (t, $J = 4.6$ Hz, *o*-Ph), 133.84 (t, $J = 5.3$ Hz, *o*′-Ph), 130.52 (t, $J = 18.1$ Hz, *i*-Ph), 130.37 (s, *p*-Ph), 129.95 (t, $J = 22$ Hz, *i*′-Ph), 129.65 (s, *p*′-Ph), 127.99 (m, *m*-Ph and *m*′-Ph), 58.76 (N*C*H$_2$CH$_2$CH$_2$-CH$_3$), 28.67 (t, $J_{PC} = 20.7$ Hz, P*C*H$_2$), 24.31 (NCH$_2$*C*H$_2$CH$_2$CH$_3$), 19.87 (NCH$_2$CH$_2$*C*H$_2$CH$_3$), 13.81 (NCH$_2$CH$_2$CH$_2$*C*H$_3$), 12.55 (t, $J_{PC} = 24.5$ Hz, Si*C*H$_2$), 2.21 (SiCH$_3$). ^{31}P NMR (121.6 MHz, $CDCl_3$, 24.4 °C): δ 39.11. UV−visible (λ_{max}, nm, CH_2Cl_2 (ϵ)): 232 (28 000). Anal. Calcd for $C_{50}H_{82}N_2O_4OsP_2SSi_2$: C, 53.83; H, 7.41; N, 2.51; S, 2.87. Found C, 51.05; H, 7.53; N, 2.57; S, 3.18. Melting point: 150−152 °C.

Reaction of 1a with Excess 30% H_2O_2. A solution of **1a** (0.048 g, 0.065 mmol) in 20 mL of CH_2Cl_2 was stirred with two drops of 30% H_2O_2. The purple solution changed to yellow-green, black-green, purple-blue, and finally a brilliant cobalt blue over the course of 5 min. The organic layer was separated, and the solvent was removed under vacuum. The oil was crystallized from chloroform/pentane at −30 °C to yield dark blue crystals of [N(*n*-Bu)$_4$]$_2$[OsCrO$_5$] (0.015 g, 0.019 mmol, 57%). The solid material decomposed at room temperature to a white solid. IR (KBr, cm^{-1}): 2360, 2341, 1474, 1458, 949, 902, 668. ^{1}H NMR (300 MHz, $CDCl_3$, 19.5 °C): δ 0.99 (m, 12H, NCH$_2$CH$_2$-CH$_2$C*H*$_3$), 1.42 (m, 8H, NCH$_2$CH$_2$C*H*$_2$CH$_3$), 1.62 (m, 8H, NCH$_2$C*H*$_2$-CH$_2$CH$_3$), 3.20 (m, 8H, NC*H*$_2$CH$_2$CH$_2$CH$_3$). UV−visible (λ_{max}, nm, CH_2Cl_2): 572. Anal. Calcd for $N_2C_{32}H_{72}OsCrO_5$: C, 47.62; H, 8.99; N, 3.47. Found: C, 47.38; H, 9.06; N, 3.79.

Reaction of 1b with 2 Equiv of 30% H_2O_2. To a stirred solution of **1b** (0.045 g, 0.054 mmol) in 15 mL of CH_3CN was added 12 μL of a 30% hydrogen peroxide solution in water. The color slowly changed from purple to orange. Solvent was evaporated under vacuum, and the residue was dissolved in 1 mL of CH_2Cl_2 and 5 mL of $(C_2H_5)_2O$. Hexane was layered on the solution until orange crystals began to form. IR (KBr, cm^{-1}): 3058 (w, phenyl ν_{CH}), 2951 (w, ν_{CH}), 2889 (w, ν_{CH}), 1438 (s, δ_{CH}), 1109 (s, δ_{PC} and ν_{OsN}), 940 (b, ν_{CrO}), 890 (m, ν_{OO}), 834 (m, γ_{SiCH_3}), 723 (m, δ_{ar-CH}), 690 (m, δ_{ar-CH}), 527 (m). ^{1}H NMR (300 MHz, C_6D_6): δ 3.55 (m, 1H, OsCH^c*H*^{d}), 2.88 (br, 1H, OsC*H*^{c}H^d), 2.48 (br, 1H, OsCH^a*H*^{b}), 1.37 (br, 1H, OsC*H*^{a}H^b), 0.46 (s, 9H, SiCH$_3$), 0.43 (s, 9H, SiCH$_3$). UV−visible (λ_{max}, nm, CH_3CN): 466.

Preparation of $C_6H_5CD_2OH$. To a 200-mL, two-necked round-bottomed flask equipped with a stir bar, a dropping funnel, and reflux condenser were added $LiAlD_4$ (1.7 g, 0.0405 mol) and 30 mL of $(C_2H_5)_2O$. A solution of $PhCO_2C_2H_5$ (10 g, 0.066 mol) in 15 mL of $(C_2H_5)_2O$ was added slowly with vigorous stirring at such a rate that the solvent refluxed gently. After the addition was completed, the mixture was heated to reflux for 3 h. Ethyl acetate (5 mL) and then aqueous HCl (6 M, 45 mL) were added. The organic layer was dried over K_2CO_3. The $(C_2H_5)_2O$ was removed under vacuum, and the product (5.8 g, 80%) was purified by distillation under reduced pressure. ^{1}H NMR ($CDCl_3$, 200 MHz, 296 K): δ 7.25 (m, 5H, C_6H_5). 2.02 (m, 1H, OH). Anal. Calcd for $C_6H_5CD_2OH$: C, 76.26; H, 7.46. Found: C, 75.68. H, 7.32.

Preparation of PhCH(D)OH. To a solution of PhCHO (6.26 g, 59 mmol) in 30 mL of THF was added $LiAlD_4$ (1.0 g, 23.8 mmol). The mixture was heated to reflux and stirred overnight. Aqueous HCl (10 mL, ∼4 M) was then added to hydrolyze the aluminum alkoxide and any unreacted $LiAlD_4$. The reaction mixture was filtered and the filtrate washed with $(C_2H_5)_2O$. The filtrate was distilled. The fraction boiling at 205−206 °C was collected. ^{13}C{^{1}H} ($CDCl_3$, 125.76 MHz, 20 °C): δ 140.8 (s), 127.2 (s), 128.2 (s) 126.6 (s), 65.4 (t, $J_{CD} = 20$ Hz).

Reaction 1a with $C_6H_5CD_2OH$. In a 5-mm NMR tube, **1a** (0.014 mg, 0.02 mmol) and $PhCD_2OH$ (2.0 μL, 0.02 mmol) were dissolved in 0.5 mL of C_6H_6. The solution was heated to 70 °C for 10 h under air. CD_3CN (1.5 μL, 0.03 mmol) was injected to the solution as a internal standard, and the deuterated species were analyzed by ^{2}H NMR spectroscopy. ^{2}H NMR (C_6H_6, 46 MHz, 293 K): δ 9.62 (s, 0.18D, PhCDO), 4.78 (s, 0.36D, D_2O/HOD).

Reaction of 1a with C_6H_5CDHOH. A solution of **1a** (0.018 g, 0.024 mmol) and PhCH(D)OH (0.050 mL, 0.048 mmol) in 0.75 mL of C_6D_6 was added to a 5-mm NMR tube, and the tube was capped with a septum. Dry oxygen was added to the mixture via a syringe adapter, and the solution was heated to 70 °C. After 2 h, a ^{1}H NMR spectrum was obtained. All of the alcohol had been converted to aldehyde. The ratio of PhCHO to PhCDO was 1:1.9 by integration.

Reaction of 1a with $PhCH_2OH$. A solution of **1a** (0.025 g, 0.034 mmol) in 5 mL of $PhCH_3$ and 1.0 equiv of $PhCH_2OH$ (3.5 mL, 0.034 mmol) was prepared under N_2. The purple solution was heated to 70 °C with magnetic stirring. After 2 h, the color of the solution had changed from purple to green. UV−visible (λ_{max}, nm, $PhCH_3$ (ϵ)): 560 (138). IR ($PhCH_3$, cm^{-1}): 1545 (s), 1400 (s, δ_{CH}), 1375 (s, δ_{CH}), 1240 (s, δ_{Si-C}), 1123 (s, ν_{Os-N}), 1026 (s), 954 (vs, $\nu_{Cr=O}$), 832 (vs, $\nu_{Cr=O}$), 728 (s), 717 (s). ESR ($PhCH_3$, 293 K): 2060 G, $g_1 = 3.3842$; 3525 G, $g_2 = 1.9803$.

The green solution was heated to 70 °C, and O_2 was bubbled through the solution for 2 h. Some black solid precipitated from the solution. The color of the solution gradually changed from green to purple. The IR and UV−visible spectra of purple species show that it is identical with **1a**. IR (toluene, cm^{-1}): 1110 (s, ν_{Os-N}), 950 (s, $\nu_{Cr=O}$), 927 (s, $\nu_{Cr=O}$). UV−visible (λ_{max}, nm, toluene): 502. Based on the absorbance of this band, 45% (0.015 mmol) of **1a** was regenerated. Hexane was added to the toluene solution, and it was cooled to −30 °C. Purple crystals of **1** (0.009 g, 0.012 mmol, 36%) were collected by filtration.

Catalytic Oxidation of Alcohols by 1a. (a) Variation of Alcohol. For each reaction, a solution of **1a** (0.0082 g, 0.011 mmol), alcohol (0.22 mmol), and anisole (12.2 μL, 0.10 mmol) in 4.0 mL of $PhCH_3$

was prepared and added to a 15-mL flask equipped with a magnetic stir bar and condenser. Each solution was heated to 70 °C and stirred at that temperature under air for 3 h. The yield and identity of oxidized product were determined by GC analysis and comparison with authentic samples.

(b) Competition between Primary and Secondary Alcohols. For each reaction, a solution of **1a** (0.008 g, 0.01 mmol), primary alcohol (0.23 mmol), secondary alcohol (0.023 mmol), and anisole (12.2 μL, 0.10 mmol) in 4.0 mL of $PhCH_3$ was prepared and added to a 25-mL flask equipped with a magnetic stir bar and condenser. Each solution was stirred at 70 °C under air for 3 h. The ratio of aldehyde/ketone was obtained by GC analysis.

Reaction of 1a with $^{17}O_2$. A solution of **1a** (0.020 g, 0.027 mmoL) and $PhCH_2OH$ (2.8 μL, 0.027 mmol) in 3 mL of C_6H_6 was injected through a septum into a flask containing 25 mL of $^{17}O_2$ (1 mmol, 49% label). The vessel was sealed and heated to 70 °C for 24 h. The purple solution was then concentrated to 1 mL under vacuum, and C_6H_{14} was added. Purple crystals (0.008 g, 40%) of **1a** were collected and dried under vacuum. ^{17}O NMR (C_6H_6, 40.7 MHz, 293 K): δ 537 ppm. IR (KBr, cm^{-1}): 1111 (s, $\nu_{Os\equiv N}$), 948 (vs, $\nu_{Cr=O}$), 928 (vs, $\nu_{Cr=O}$).

A solution of **1a** (0.22 g, 0.32 mmol) and $PhCH_2OH$ (90 μL, 0.86 mmol) in 1.5 mL of C_6D_6 was injected through a septum into a flask containing 100 mL of $^{17}O_2$ (49% label). The vessel was sealed and heated to 60 °C for 12 h. A sample was transferred to a 5-mm NMR tube, and a $^{13}C\{^1H\}$ NMR spectrum was obtained.$^{13}C\{1H\}$ NMR (C_6D_6, 125.76 MHz, 293 K): δ 196 (Ph*C*HO), 144−120 (Ph), 65 (Ph*C*H_2-OH), 60 (N*C*$H_2CH_2CH_2CH_3$), 25 (NCH_2*C*$H_2CH_2CH_3$), 20 (NCH_2-CH_2*C*H_2CH_3), 14 ($NCH_2CH_2CH_2$*C*H_3), 2 ($SiCH_3$). The spectrum was broad, but resonances due to **1a**, PhCHO, and $PhCH_2OH$ were present. ^{17}O NMR (C_6H_6, 40.7 MHz, 293 K): δ 565 (sh, low intensity), 537 (br, Os−O−Cr). Additional $PhCH_2OH$ (90 μL, 0.86 mmol) was added to the sample in the NMR tube, and it was heated to 70 °C under O_2 for 2 h. ^{17}O NMR (C_6H_6, 40.7 MHz, 293 K): δ 565 (sh), 537 (br s, Os−O−Cr), 0 (br s, H_2O).

Catalytic Oxidation of $PhCH_2OH$ by 1a. (a) Variation of Solvent. For each reaction, a solution of **1a** (0.013 g, 0.0176 mmol) and $PhOCH_3$ (19.3 μL, 0.176 mmol) in 0.6 mL of solvent was added to a 5-mm NMR tube under air. The temperature was maintained at 40 °C in the probe of the NMR spectrometer, and ^1H NMR spectra were recorded and stored every 2 min. The observed rate constant was obtained from the slope of a plot of −ln [$PhCH_2OH$] vs time (s).

(b) Variation of Catalyst Concentration. A 2.0-mL solution of **1a** (0.040 g, 0.05 mmoL) and anisole (64 μL, 0.6 mmol) in C_6D_6 was prepared in a volumetric flask. To each of four 5-mm NMR tubes was added a quantity of this solution, 0.2 mmol of $PhCH_2OH$, and sufficient C_6D_6 to give a total volume of 0.60 mL. The temperature of the NMR spectrometer probe was maintained at 70 °C, and a ^1H NMR spectrum was collected and stored every 2 min. The observed rate constant was obtained from the slope of a plot of −ln [$PhCH_2OH$] vs time (s). The second-order rate constant, 2.9×10^{-2} M^{-1} s^{-1}, was obtained from the slope of a plot of k_{obs} vs [**1a**].

(c) Variation in O_2 Concentration. A solution of **1a** (0.10 g, 0.136 mmol), $PhCH_2OH$ (0.294 g, 2.72 mmol), and $PhOCH_3$ (0.015 g, 0.136 mmol,) in 25.0 mL of $PhCH_3$ was prepared in a volumetric flask. Each 2.5-mL sample was transferred to a flask equipped with a gas inlet, stir bar, and condenser. The temperature was maintained at 70 °C, and a mixture of N_2 and O_2 was bubbled through the solution. The total pressure was 1 atm. Aliquots were taken by syringe every 2 min and analyzed by GC. The observed rate constants, k_{obs}, were obtained from plots of −ln [$PhCH_2OH$] vs time (s). The second-order rate constants, k, were obtained by dividing k_{obs} by [**1a**].

(d) Variation in Temperature. To each 5-mm NMR tube was added 0.50 mL of a C_6D_6 solution of **1a** (0.044 g, 0.006 mmol), $PhCH_2OH$ (0.020 mmol), and $PhOCH_3$ (0.06 mmol). Each solution, open to air, was placed in the probe of the NMR spectrometer that had been maintained at the temperature of interest. A ^1H NMR spectrum was collected and stored every 2 min. Concentrations of PhCHO, $PhCH_2$-OH, and $PhOCH_3$ were obtained by integration of these spectra. The observed rate constant was obtained from the slope of the plot of −ln [$PhCH_2OH$] vs time (s). The equation of the line from the plot shown in Figure 6 is $\ln(k/T) = 65.7 - 53310(1/T)$.

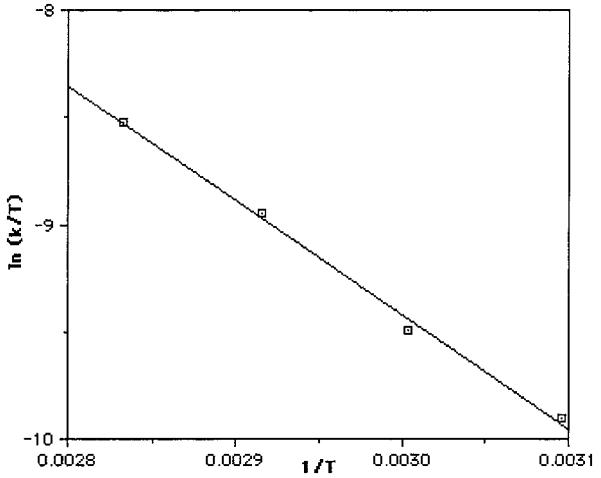

Figure 6. Temperature dependence of the rate of $PhCH_2OH$ oxidation by **1a**.

Rate of Oxidation of $PhCH_2OH$ by 2. To a 15-mL flask equipped with a magnetic stir bar and condenser were added **2** (0.002 g, 0.003 mmol), $PhCH_2OH$ (6.7 μL, 0.064 mmol), $PhOCH_3$ (3.4 μL, 0.026 mmol), and 2 mL of $PhCH_3$. The flask was maintained at 72 °C, and the solution was stirred vigorously under air. Samples of the solution were removed every 20 min, and the concentrations of $PhCH_2OH$, PhCHO, and $PhOCH_3$ were analyzed by GC. The observed rate constant, 5.7×10^{-4} s^{-1}, was obtained from the slope of a plot of −ln [$PhCH_2OH$] vs time (s).

Rate of Oxidation of $PhCH_2OH$ by 4. To a 15-mL flask equipped with a magnetic stir bar and condenser were added **2** (0.002 g, 0.003 mmol), $PhCH_2OH$ (6.7 μL, 0.064 mmol), $PhOCH_3$ (3.4 μL, 0.026 mmol), and 2 mL of nitromethane. The flask was maintained at 72 °C, and the solution was stirred vigorously under air. Samples of the solution were removed every 20 min, and the concentrations of $PhCH_2$-OH, PhCHO, and $PhOCH_3$ were analyzed by GC. The observed rate constant, 9.8×10^{-5} s^{-1}, was obtained from the slope of a plot of −ln [$PhCH_2OH$] vs time (s).

Rate of Oxidation of $PhCH_2OH$ by 5. Benzyl alcohol (0.1933 M) and **5** (0.010 M) were added to a small flask containing $PhOCH_3$ (1 μL as internal standard) and $PhCH_3$. The reaction was stirred under air at 65 °C. Aliquots were removed and analyzed by gas chromatography at intervals. A plot of −ln [$PhCH_2OH$] vs time (s) gave a slope, or $k_{obs} = 6.46 \times 10^{-5}$ s^{-1}.

Oxidation of Alcohols by 5. For each reaction, **5** (7.9 mg, 0.011 mmoL), alcohol (0.23 mmol), and $PhOCH_3$ (10.0 μL, 0.092 mmol) in 4.0 mL of $PhCH_3$ was added to a 15-mL flask equipped with a stir bar and condenser. The mixture was heated under air for 24 h. Aliquots were taken periodically, and the concentrations of alcohol, oxidized product(s), and $PhOCH_3$ were determined by GC analysis.

Competition by 5 for the Oxidation of $PhCH_2OH$ and $PhCH(OH)CH_3$. A solution of **5** (0.0013 g, 0.0018 mmol), $PhCH_2OH$ (4.3 μL, 0.041 mmol), and $PhCH(OH)CH_3$ (5 μL, 0.041 mmol) in 0.72 mL of $PhCH_3$ was stirred at 67 °C under air for 1 h (20% completion). The ratio of products was determined by GC analysis (aldehyde/ketone = 7:1).

Solvent Effects on the Oxidation of Benzyl Alcohol. For each reaction, a solution of **5** (0.007 g, 0.010 mmol), $PhCH_2OH$ (0.021 g, 0.193 mmol), and $PhOCH_3$ (1.0 μL, 0.009 mmol) in 1.0 mL of solvent was added to a small flask under air. The reaction was stirred under air at 60−65 °C. Aliquots were removed and analyzed by gas chromatography at intervals. The observed rate constant was obtained from the slope of a plot of −ln [$PhCH_2OH$] vs time (s).

Dependence of the Rate on [5]. A solution of **5**, $PhCH_2OH$ (0.019 g, 0.180 mmol), and $PhOCH_3$ (2.2 μL, 0.020 mmol) in 1.0 mL of $PhCH_3$ was added to a small flask. The reaction was stirred under air at 65 °C. Aliquots were removed and analyzed by gas chromatography at intervals. The observed rate constant was obtained from the slope of a plot of −ln [$PhCH_2OH$] vs time (s). For 0.00179 M **5**, $k = 10.3 \times 10^{-5}$ s^{-1}, and for 0.000447 M **5**, $k = 2.30 \times 10^{-5}$ s^{-1}.

Anaerobic Reaction of 5 with $PhCH_2OH$. Under N_2, $PhCH_2OH$ (0.80 μL, 0.00773 mmol) and **5** (0.000958 mmol) were dissolved in dry, degassed C_6D_6 and transferred to an NMR tube. The NMR tube was free−pump−thawed three times and then flame-sealed under vacuum. The tube was heated at 95 °C for 48 h. The ratio of aldehyde (1H) to alcohol (28H) protons was measured by ^{1}H NMR spectroscopy.

The measurement was repeated with $PhCH_2OH$ (0.99 μL, 0.00958 mmol) and **5** (0.000958 mmol) under the same conditions. The ratio of aldehyde (1H) to alcohol (26H) protons was measured by ^{1}H NMR spectroscopy.

Reaction of 5 with PhCHO and H_2O. Under N_2, PhCHO (2.0 μL, 0.0197 mmol) and **5** (0.00120 mmol) were dissolved in dry, degassed C_6D_6 and transferred to an NMR tube. The tube was heated at 80 °C for 1 h. Water (25 μL) was added. After the tube was heated an additional 48 h, the ratio of alcohol α protons (3H) to aldehyde α protons (1H) was measured by proton NMR (1.57).

Reaction of 7a with O_2. A sample of **7a** (0.010 g, 0.009 mmol) was dissolved in 0.75 mL of $CDCl_3$ in air. After 7 days, the solution had turned from yellow to purple, and ^{1}H NMR indicated that **1a** was now the major organometallic species present in solution. The phosphorus-containing material was entirely $Ph_2P(O)CH_2CH_2P(O)Ph_2$, identical to a pure sample of the oxidized phosphine. MS (EI, 70 eV, *m*/*z* (relative abundance)): 429 ($M^+ - H$, 1.02), 353 ($M^+ - Ph$, 100), 229 ($Ph_2P(O)CH_2CH_2^+$, 64.87), 201 ($P(O)Ph_2^+$, 32.35), 77 (Ph^+, 37.87). ^{1}H NMR (300 MHz, $CDCl_3$, 20.0 °C): δ 2.52 (d, 4H, J = 2.5 Hz, CH_2), 7.4−7.6 (m, Ph), 7.6−7.8 (m, Ph).

Reactions of Other Osmium Complexes, dppe, and O_2. The following compounds were tested as catalysts for the oxidation of dppe with O_2: $[N(n\text{-}Bu)_4][Os(N)(CH_2SiMe_3)_2(SO_4)]$, $[N(n\text{-}Bu)_4][Os(N)(CH_2SiMe_3)_2(SO_4)(dppe)]$, $[N(n\text{-}Bu)_4][Os(N)(CH_2SiMe_3)_2(CO_3)]$, $[Os(N)(CH_2SiMe_3)_2(dppe)(NCMe)][BF_4]$, $[Os(N)(CH_2SiMe_3)_2(dppe)][BF_4]$, and $Os(N)(CH_2SiMe_3)_2Cl(dppe)$. In each reaction, the osmium compound (0.014−0.017 mmol) and dppe (0.008 mg, 0.02 mmol) were dissolved in 0.75 mL of C_6D_6. The sample was exposed to air and was warmed to 75 °C for 24 h. The quantity of $Ph_2P(O)CH_2CH_2P(O)Ph_2$ was determined by integration of the ^{1}H NMR spectrum. $[N(n\text{-}Bu)_4][Os(N)(CH_2SiMe_3)_2(SO_4)]$, $[N(n\text{-}Bu)_4][Os(N)(CH_2SiMe_3)_2(SO_4)(dppe)]$, and $[N(n\text{-}Bu)_4][Os(N)(CH_2SiMe_3)_2(CO_3)]$ converted 0.30−0.40 equiv of dppe to the phosphine oxide. The other compounds either did not react or converted only a trace of the dppe to an oxidized product.

Reaction of dppe and O_2. Dppe (0.008 mg, 0.02 mmol) was dissolved in 0.75 mL of C_6D_6, and a ^{1}H NMR spectrum was obtained. The mixture was heated at 60−70 °C and monitored by ^{1}H NMR spectroscopy. After 3 d, only a trace of oxide was formed.

Method for the Catalysis of dppe Oxidation by 7a. Solutions of dppe, **7a**, and $PhOCH_3$ (2 μL, internal standard) in 0.75 mL of $C_6D_5CD_3$ were prepared in 5-mm NMR tubes in air. Each reaction mixture was maintained at a constant temperature, and the product formation was monitored by ^{1}H NMR spectroscopy. A preacquisition delay of 7.5 s was used to allow complete relaxation of all nuclei.

Stoichiometric Addition of $^{18}O_2$ to 7a. A solution of **7a** (0.030 g, 0.026 mmol) in 15 mL of $PhCH_3$ was degassed by three successive freeze−pump−thaw cycles. The solution was frozen in $N_{2(l)}$, and 20 mL of $^{18}O_2$ (95%) was added by gastight syringe. The mixture was warmed to 70 °C with magnetic stirring and maintained at that temperature for 2 h. The solution changed from yellow to purple over this time, indicating formation of **1a**. The isotope ratio of the intense $[Ph_2P(O)CH_2CH_2P(O)Ph]^+$ peak in the EI mass spectrum was analyzed (*m*/*z* (relative abundance)): 353 (100), 354 (35.30), 355 (9.99), 356 (2.10), 357 (1.82), 358 (0.87).

Addition of $^{18}O_2/^{16}O_2$ to 7a and dppe. A solution of **7a** (0.020 g, 0.018 mmol) and dppe (0.070 g, 0.18 mmol) in 15 mL of $PhCH_3$ in a 100-mL flask was degassed by three successive freeze−pump−thaw cycles. The solution was frozen in $N_{2(l)}$, and the flask was filled with a mixture of $^{18}O_2/^{16}O_2$ (ratio 13:37). The reaction mixture was stirred at 70−80 °C for 2 h. The isotope ratio of the intense $[Ph_2P(O)CH_2CH_2P(O)Ph]^+$ peak in the EI mass spectrum was analyzed (*m*/*z* (relative abundance)): 353 (100), 354 (24.32), 355 (85.31), 356 (18.77), 357 (23.09), 358 (5.59).

Acknowledgment. We gratefully acknowledge the financial support of the National Science Foundation (CHE 95-26350) in this work. NMR spectra were obtained in the Varian Oxford Instrument Center for Excellence in NMR Laboratory. Funding for this instrumentation was provided in part from the W. M. Keck Foundation, the National Institutes of Health (PHS 1 S10 RR10444-01), and the National Science Foundation (NSF CHE 96-10502). Purchase of the Siemens Platform/CCD diffractometer by the School of Chemical Sciences was supported by National Science Foundation (CHE 9503145). We thank Scott R. Wilson and Theresa Prussak-Wieckowska for collection of crystal data and helpful discussions in the solving of the crystal structures.

Supporting Information Available: For **2** and **6**, tables of additional crystal data collection and refinement parameters, atomic coordinates, thermal parameters, tables of distances and angles, and tables of additional kinetic data (PDF). This material is available free of charge via the Internet at http://pubs.acs.org.

JA982171Y